

Follicular Dendritic Cell-Specific Prion Protein (PrP^C) Expression Alone Is Sufficient to Sustain Prion Infection in the Spleen

Laura McCulloch¹, Karen L. Brown¹, Barry M. Bradford¹, John Hopkins¹, Mick Bailey², Klaus Rajewsky³, Jean C. Manson¹, Neil A. Mabbott^{1*}

1 The Roslin Institute & Royal (Dick) School of Veterinary Sciences, University of Edinburgh, Midlothian, United Kingdom, **2** Division of Veterinary Pathology, Infection and Immunity, School of Clinical Veterinary Science, University of Bristol, Avon, United Kingdom, **3** Program in Cellular and Molecular Medicine, Children's Hospital, and Immune Disease Institute, Harvard Medical School, Boston, Massachusetts, United States of America

Abstract

Prion diseases are characterised by the accumulation of PrP^{Sc}, an abnormally folded isoform of the cellular prion protein (PrP^C), in affected tissues. Following peripheral exposure high levels of prion-specific PrP^{Sc} accumulate first upon follicular dendritic cells (FDC) in lymphoid tissues before spreading to the CNS. Expression of PrP^C is mandatory for cells to sustain prion infection and FDC appear to express high levels. However, whether FDC actively replicate prions or simply acquire them from other infected cells is uncertain. In the attempts to-date to establish the role of FDC in prion pathogenesis it was not possible to dissociate the *Prnp* expression of FDC from that of the nervous system and all other non-haematopoietic lineages. This is important as FDC may simply acquire prions after synthesis by other infected cells. To establish the role of FDC in prion pathogenesis transgenic mice were created in which PrP^C expression was specifically “switched on” or “off” only on FDC. We show that PrP^C-expression only on FDC is sufficient to sustain prion replication in the spleen. Furthermore, prion replication is blocked in the spleen when PrP^C-expression is specifically ablated only on FDC. These data definitively demonstrate that FDC are the essential sites of prion replication in lymphoid tissues. The demonstration that *Prnp*-ablation only on FDC blocked splenic prion accumulation without apparent consequences for FDC status represents a novel opportunity to prevent neuroinvasion by modulation of PrP^C expression on FDC.

Citation: McCulloch L, Brown KL, Bradford BM, Hopkins J, Bailey M, et al. (2011) Follicular Dendritic Cell-Specific Prion Protein (PrP^C) Expression Alone Is Sufficient to Sustain Prion Infection in the Spleen. *PLoS Pathog* 7(12): e1002402. doi:10.1371/journal.ppat.1002402

Editor: Jason Bartz, Creighton University, United States of America

Received: June 15, 2011; **Accepted:** October 11, 2011; **Published:** December 1, 2011

Copyright: © 2011 McCulloch et al. This is an open-access article distributed under the terms of the Creative Commons Attribution License, which permits unrestricted use, distribution, and reproduction in any medium, provided the original author and source are credited.

Funding: This work was supported by project (Grant numbers BB/526741-1 and BBS/E/R/00001813) and Institute Strategic Grant funding from the UK Biotechnology and Biological Sciences Research Council. The funders had no role in study design, data collection and analysis, decision to publish, or preparation of the manuscript.

Competing Interests: The authors have declared that no competing interests exist.

* E-mail: neil.mabbott@roslin.ed.ac.uk

Introduction

Prion diseases (Transmissible spongiform encephalopathies; TSE) are sub-acute neurodegenerative diseases that affect both humans and animals. Many prion diseases, including natural sheep scrapie, bovine spongiform encephalopathy, chronic wasting disease in mule deer and elk, and kuru and variant Creutzfeldt-Jakob disease in humans, are acquired by peripheral exposure (eg: orally or via lesions to skin or mucous membranes). After peripheral exposure prions accumulate first upon follicular dendritic cells (FDC) as they make their journey from the site of infection to the CNS (a process termed, *neuroinvasion*) [1–7]. FDC are a unique subset of stromal cells resident within the primary B cell follicles and germinal centres of lymphoid tissues [8]. Prion accumulation upon FDC is critical for efficient disease pathogenesis as in their absence neuroinvasion are impaired [1–4]. From the lymphoid tissues prions invade the CNS via the peripheral nervous system [9].

During prion disease aggregations of PrP^{Sc}, an abnormally folded isoform of the cellular prion protein (PrP^C) accumulate in affected tissues. Prion infectivity co-purifies with PrP^{Sc} [10] and is considered to constitute the major, if not sole, component of

infectious agent [11]. Host cells must express cellular PrP^C to sustain prion infection [12] and FDC appear to express high levels of PrP^C on the cell membrane in uninfected mice [13,14]. Although prion neuroinvasion from peripheral sites of exposure is dependent upon the presence of FDC in lymphoid tissues, it is not known whether FDC actually replicate prions themselves. FDC characteristically trap and retain native antigen on their surfaces for long periods in the form of immune complexes, consisting of antigen-antibody and/or complement components. Prions are also considered to be acquired by FDC as complement-opsonized immune complexes [15–18]. Thus, during prion infection FDC might simply trap and retain PrP^{Sc}-containing immune complexes on their surfaces following synthesis by other infected cells such as neurones.

Many cell types including classical DC, lymphocytes, mast cells, platelets, reticulocytes and epithelial cells secrete membrane vesicles termed exosomes that are enriched in cell-specific protein [19,20]. Although the functions of exosomes are uncertain FDC can bind them on their surfaces. These microvesicles permit FDC to passively acquire and display proteins on their surfaces that they do not express at the mRNA level [21]. Studies have shown that prions only accumulated in the spleens of mice in which the FDC-

Author Summary

Prion diseases are infectious neurological disorders and are considered to be caused by an abnormally folded infectious protein termed PrP^{Sc}. Soon after infection prions accumulate first upon follicular dendritic cells (FDC) in lymphoid tissues before spreading to the brain where they cause damage to nerve cells. Cells must express the normal cellular prion protein PrP^C to become infected with prions. However, whether FDC are infected with prions or simply acquire them from other infected cells is unknown. To establish the role of FDC in prion disease PrP^C expression was specifically “switched on” or “off” only on FDC. We show that PrP^C-expressing FDC alone are sufficient to sustain prion replication in the spleen. Furthermore, prion replication is blocked in the spleen when PrP^C-expression is switched off only on FDC. These data definitively demonstrate that FDC are the essential sites of prion replication in lymphoid tissues.

containing stromal compartment expressed PrP^C [13,14]. However, in each of those studies it was not possible to dissociate the *Pmp* expression status of the FDC from that of the nervous system and all other host-derived non-haematopoietic and stromal cell populations [13,14,22]. This is important as prion infection can occur within inflammatory PrP^C-expressing stromal cells that are distinct from FDC [23]. Furthermore, as both PrP^C and PrP^{Sc} can be released from cells in association with exosomes [20] FDC may passively acquire PrP^C and prions after release in exosomes from other infected cells [24,25].

No therapies are available to treat prion diseases. A thorough characterization of the host cells that are infected by prions is imperative for the identification of candidate molecular targets for therapeutic intervention, the development of useful pre-clinical diagnostics and to aid our understanding of the risk of transmission. To definitively determine the role of FDC in prion pathogenesis, two unique compound transgenic mouse models were created in which PrP^C expression was specifically “switched on” or “switched off” only on FDC. These mice were then used to establish: i) whether FDC express PrP^C or simply acquire it from other host cells; and ii) whether FDC amplify prions, or simply acquire them from other infected host cells. Our data clearly show that PrP^C-expressing FDC alone are sufficient to sustain prion replication in the spleen. Furthermore, prion replication in the spleen is blocked in mice in which PrP^C-expression is specifically ablated only on FDC.

Results

Mice expressing Cre recombinase specifically in FDC

To study FDC-specific gene function transgenic mice were used that expressed Cre recombinase under the control of the *Cr2* locus (CD21-Cre mice) which directs expression in FDC and mature B cells [26,27]. First the cellular specificity of the Cre recombination was assessed by crossing the CD21-Cre mice with the ROSA26^{lox/lox} reporter strain [28]. Histological analysis showed efficient *LacZ* expression indicative of Cre-mediated gene recombination in FDC and B cell follicles in the spleens, lymph nodes and Peyer’s patches of CD21-Cre ROSA26^{lox/lox} mice (Figure 1A, B). No recombination was observed in FDC and mature B cells in the spleens of ROSA26^{lox/lox} reporter mice that lacked Cre expression (Figure 1B). Unlike lymphocytes, FDC do not derive from bone marrow precursors [29]. As a consequence, it is possible to mix-and-match the genotype of FDC and

lymphocytes by grafting bone marrow cells from donor mice into recipients of a different genetic background [13,14,22]. To restrict Cre-expression to FDC, adult CD21-Cre ROSA26^{lox/lox} mice were lethally γ -irradiated and 24 h later reconstituted with bone marrow from Cre-deficient C57BL/6 wild-type (WT) mice (termed WT \rightarrow CD21-Cre ROSA26^{lox/lox} mice) and tissues from six mice from each group analysed 100 days after transfusion. Using this approach, in these mice all B cells lack Cre-expression as they derive from the WT donor bone marrow, whereas the FDC express Cre as they are host-derived. Analysis of the cellular sites of *LacZ* expression in WT \rightarrow CD21-Cre ROSA26^{lox/lox} mice confirmed that Cre-mediated recombination was associated with FDC (Figure 1B). No other cellular sites of Cre-mediated recombination were observed in the spleens of WT \rightarrow CD21-Cre ROSA26^{lox/lox} mice. Furthermore, no other cellular sites of Cre-mediated recombination were observed in a wide range of non-lymphoid peripheral tissues from CD21-Cre ROSA26^{lox/lox} and WT \rightarrow CD21-Cre ROSA26^{lox/lox} (heart, liver, kidney, pancreas, ear, tongue, skeletal, muscle, ovary, uterus, bladder, testes, epididymis, sciatic nerve and spinal cord; data not shown). These data clearly demonstrate that CD21-Cre mice are a useful tool to study FDC-specific gene expression and function.

Expression of Cre recombinase by the *Cr2* promoter is not toxic to FDC

Cre toxicity can occur in some Cre transgenic mouse lines whereby Cre recombinase causes mis-recombination, DNA damage and death of Cre-expressing cells [30]. However, immunohistochemical (IHC) analysis of spleens from CD21-Cre ROSA26^{lox/lox} mice and WT \rightarrow CD21-Cre ROSA26^{lox/lox} mice showed no significant effect of Cre-expression on the status of FDC networks and B cell follicles when compared to spleens from WT control mice and ROSA26^{lox/lox} mice that lacked Cre expression (Figure 1C). Furthermore, the expression of Cre recombinase under the control of the *Cr2* locus had no observable effect on CD21/35 expression (Figure 1C).

FDC express *Pmp* and do not acquire PrP^C from neighbouring cells

Next, mice were created in which *Pmp* expression (which encodes PrP^C) was restricted only to FDC. To do so, CD21-Cre mice were first bred onto a PrP^C-deficient (*Pmp*^{-/-}) background. The resulting CD21-Cre *Pmp*^{-/-} mice were then crossed with *Pmp*^{stop/-} mice in which a floxed β -geo stop cassette was inserted into intron 2 of the *Pmp* gene upstream of exon 3 [31]. In the progeny CD21-Cre *Pmp*^{stop/-} mice, PrP^C is only expressed in cells expressing Cre recombinase (CD21-expressing FDC and mature B cells). To restrict the *Pmp*-expression to FDC, CD21-Cre *Pmp*^{stop/-} mice were lethally γ -irradiated and grafted with bone marrow from Cre-deficient *Pmp*^{stop/-} mice (*Pmp*^{stop/-} \rightarrow CD21-Cre *Pmp*^{stop/-} mice). We also performed bone marrow transfers from CD21-Cre *Pmp*^{stop/-} donors into CD21-Cre *Pmp*^{stop/-} recipients (CD21-Cre *Pmp*^{stop/-} \rightarrow CD21-Cre *Pmp*^{stop/-} mice), CD21-Cre *Pmp*^{stop/-} donors into Cre-deficient *Pmp*^{stop/-} mice (CD21-Cre *Pmp*^{stop/-} \rightarrow *Pmp*^{stop/-} mice) and *Pmp*^{+/-} donors into *Pmp*^{+/-} recipients (*Pmp*^{+/-} \rightarrow *Pmp*^{+/-} mice) as controls (Figure 2A).

Spleens, tails and blood from six mice from each group were examined 100 days after bone marrow transfusion. PCR analysis of DNA isolated from the tails, blood and spleens of mice in each group was used to confirm the presence of *Cre* (Figure 2B, upper panel) and Cre-mediated DNA recombination (Figure 2B, lower panel) within the stromal, haematopoietic or both compartments (respectively). The detection of *Cre* in the tail and spleen but not

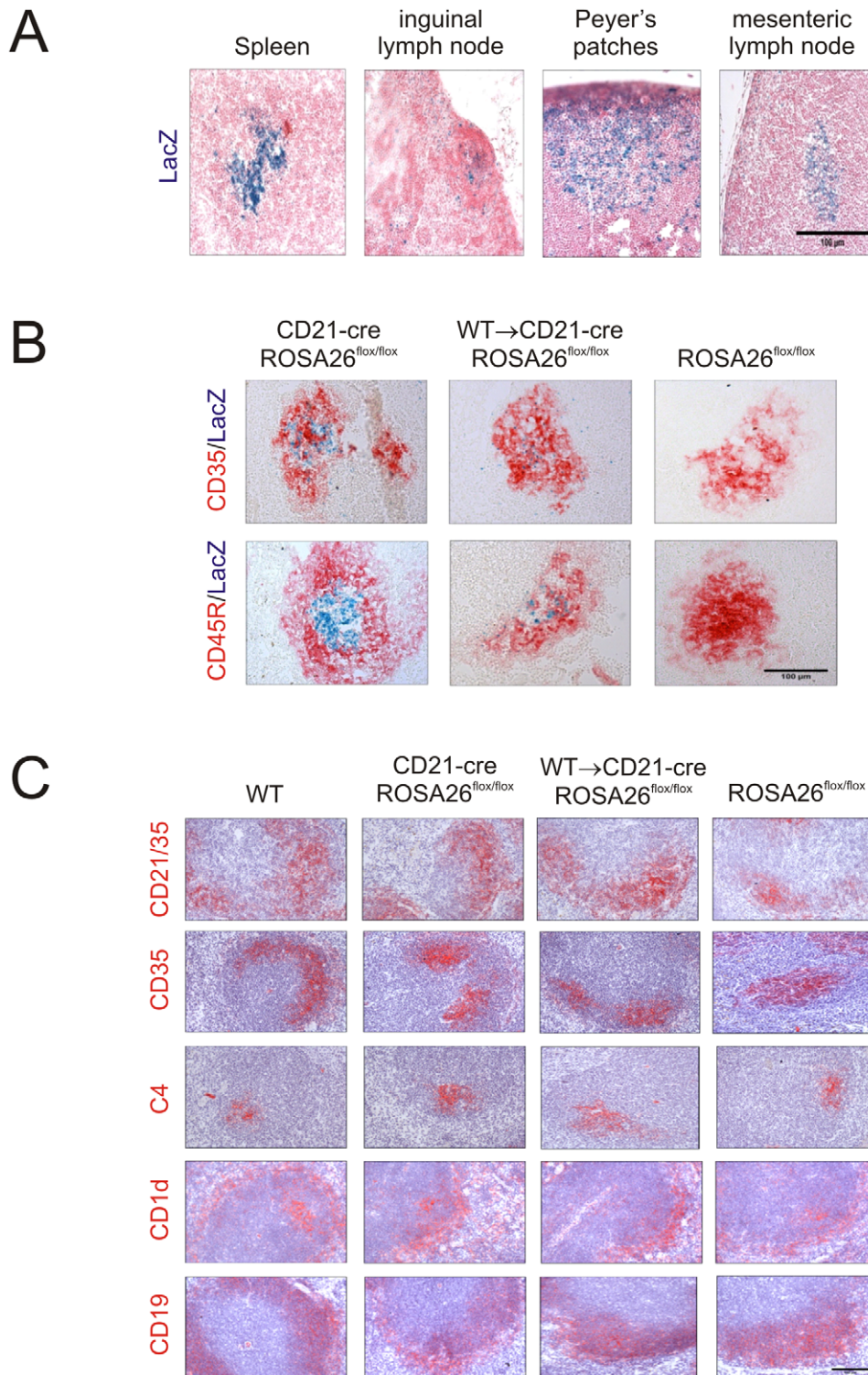


Figure 1. Cre-mediated gene recombination in FDC in the spleens, lymph nodes and Peyer's patches of CD21-Cre ROSA26^{flox/flox} mice. A) Analysis of the cellular sites of LacZ expression (blue) in the spleens, inguinal lymph nodes, Peyer's patches and mesenteric lymph nodes of CD21-Cre ROSA26^{flox/flox} mice shows Cre-mediated recombination in a focus of cells within the B cell follicles. Sections were counterstained with nuclear fast red (red). B) IHC analysis of FDC (CD35⁺ cells, upper row, red) and B cells (CD45R⁺ cells, lower row, red) confirmed that Cre-mediated LacZ expression (blue) was associated with FDC in the spleens of WT→CD21-Cre ROSA26^{flox/flox} mice. No LacZ expression was associated with FDC in spleens from ROSA26^{flox/flox} mice that lacked Cre. C) IHC analysis of the status of FDC (CD35⁺ and C4-binding cells; red) and B cells expressing CD45R, CD19, and CD1d (red) in spleens from WT, CD21-Cre ROSA26^{flox/flox}, WT→CD21-Cre ROSA26^{flox/flox} and ROSA26^{flox/flox} mice. Scale bars 100 μm. n = 6 mice/group.

doi:10.1371/journal.ppat.1002402.g001

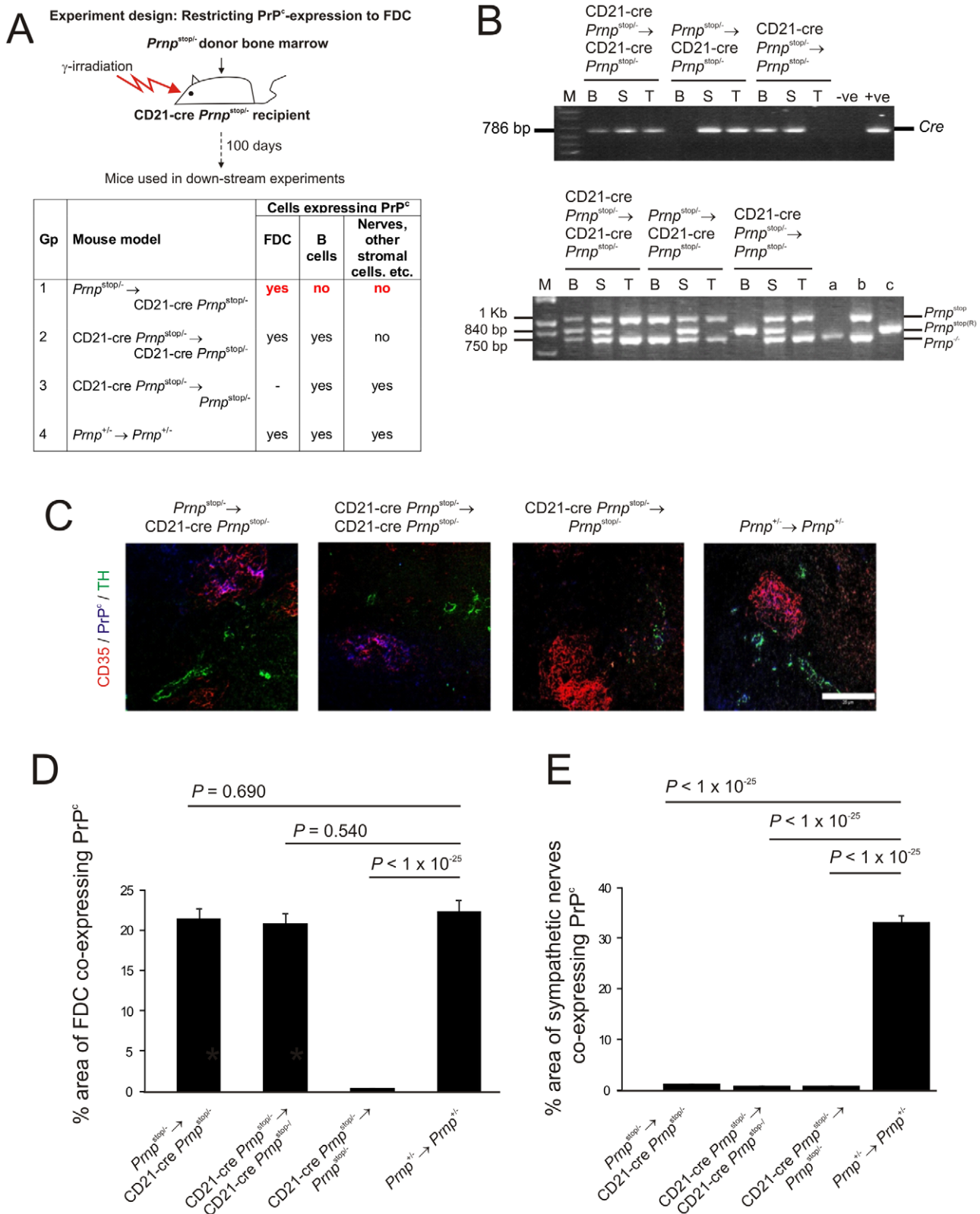


Figure 2. FDC-restricted PrP^c expression in the spleens of $Prnp^{stop/-} \rightarrow$ CD21-Cre $Prnp^{stop/-}$ mice. A) The anticipated distribution of PrP^c expression on FDC and B cells in tissues from each mouse group. B) The detection of Cre in the tail and spleen but not blood of the $Prnp^{stop/-} \rightarrow$ CD21-Cre $Prnp^{stop/-}$ mice confirmed the restriction of the Cre-expression to the stromal but not haematopoietic compartments of these mice (upper panel). Efficient Cre-mediated recombination of $Prnp^{stop}$ ($Prnp^{stop(R)}$) was restricted to the FDC-containing stromal compartment of the spleens of $Prnp^{stop/-} \rightarrow$ CD21-Cre $Prnp^{stop/-}$ mice when compared to control mice. Cre-mediated recombination by CD21-expressing lymphocytes was efficiently prevented in these mice by the irradiation and transfer of $Prnp^{stop/-}$ bone marrow as demonstrated by the lack of a $Prnp^{stop(R)}$ band in DNA extracted

from blood (lower panel). B, blood; S, spleen; T, tail; M, DNA size markers; a, b, c, control DNA samples for each transgene combination tested which were (a) *Prnp*^{-/-}, (b) *Prnp*^{stop/-} and (c) complete recombination of the stop cassette within the *Prnp*^{stop/-} allele. C) IHC analysis of PrP^C expression (blue) by FDC (CD35⁺ cells; red) and sympathetic nerves (TH⁺ cells, green) confirmed PrP^C expression was restricted to FDC in spleens of *Prnp*^{stop/-}→CD21-Cre *Prnp*^{stop/-} mice. Scale bar, 100 μm. D) Morphometric analysis confirmed that the magnitude of the PrP^C expression co-localized upon the surfaces of FDC in the spleens of *Prnp*^{stop/-}→CD21-Cre *Prnp*^{stop/-} mice was similar to that observed upon FDC in spleens from *Prnp*^{+/-}→*Prnp*^{+/-} control mice ($p < 0.690$, $n = 48$ FDC networks/group). In contrast, in the absence of Cre-recombinase expression by FDC in CD21-Cre *Prnp*^{stop/-}→*Prnp*^{stop/-} mice, PrP^C expression was substantially lower than that observed upon FDC in spleens from *Prnp*^{+/-}→*Prnp*^{+/-} control mice ($p < 1 \times 10^{-25}$, $n = 48$ FDC networks/group). E) Morphometric analysis confirmed that PrP^C expression upon the surfaces of sympathetic nerves in the spleens of *Prnp*^{stop/-}→CD21-Cre *Prnp*^{stop/-}, CD21-Cre *Prnp*^{stop/-}→CD21-Cre *Prnp*^{stop/-} and CD21-Cre *Prnp*^{stop/-}→*Prnp*^{stop/-} mice was significantly ablated when compared to that observed upon sympathetic nerves in spleens from *Prnp*^{+/-}→*Prnp*^{+/-} control mice ($p < 1 \times 10^{-25}$, $n = 48$ sympathetic nerves/group). For all panels $n = 6$ mice/group.

doi:10.1371/journal.ppat.1002402.g002

blood of the *Pmp*^{stop/-}→CD21-Cre *Pmp*^{stop/-} mice confirmed the restriction of the Cre-expression to the stromal but not haematopoietic compartments of these mice. In addition, PCR analysis also confirmed that in these mice efficient Cre-mediated recombination of the *Pmp*^{stop/-} allele was restricted to the FDC-containing stromal compartment of the spleen (Figure 2B). In *Pmp*^{stop/-}→CD21-Cre *Pmp*^{stop/-} mice the recombined *Pmp*^{stop/-} allele (*Pmp*^{stop(R)}) was detected in the spleen, but not blood and tail. Thus these data indicate that in the spleens of *Pmp*^{stop/-}→CD21-Cre *Pmp*^{stop/-} mice Cre-mediated recombination is restricted to FDC and not B cells.

As anticipated, in the spleens of *Pmp*^{+/-}→*Pmp*^{+/-} control mice high levels of PrP^C expression were observed upon FDC and tyrosine hydroxylase (TH)-positive sympathetic nerves (Figure 2C). In contrast, in the spleens of *Pmp*^{stop/-}→CD21-Cre *Pmp*^{stop/-} mice PrP^C was only expressed on FDC (Figure 2C). In the absence of Cre-recombinase expression by FDC and peripheral nerves in CD21-Cre *Pmp*^{stop/-}→*Pmp*^{stop/-} mice, PrP^C expression was not expressed by either cell population (Figure 2C).

Morphometric analysis confirmed that the amount of the PrP^C expression co-localized upon the surfaces of FDC in the spleens of *Pmp*^{stop/-}→CD21-Cre *Pmp*^{stop/-} mice was not significantly different from that observed upon FDC in spleens from *Pmp*^{+/-}→*Pmp*^{+/-} control mice ($P < 0.69$, $n = 48$ FDC/group; Figure 2D). In contrast, in the absence of Cre-recombinase expression by FDC in CD21-Cre *Pmp*^{stop/-}→*Pmp*^{stop/-} mice, PrP^C expression was substantially lower than that observed upon FDC in spleens from *Pmp*^{+/-}→*Pmp*^{+/-} control mice ($P < 1 \times 10^{-25}$, $n = 48$; Figure 2D). Morphometric analysis also confirmed that PrP^C expression upon the surfaces of sympathetic nerves in the spleens of *Pmp*^{stop/-}→CD21-Cre *Pmp*^{stop/-}, CD21-Cre *Pmp*^{stop/-}→CD21-Cre *Pmp*^{stop/-} and CD21-Cre *Pmp*^{stop/-}→*Pmp*^{stop/-} mice was significantly ablated when compared to that observed upon sympathetic nerves in spleens from *Pmp*^{+/-}→*Pmp*^{+/-} control mice ($p < 1 \times 10^{-25}$, $n = 48$ sympathetic nerves/group). Together, these data confirm that in the spleens of *Pmp*^{stop/-}→CD21-Cre *Pmp*^{stop/-} mice PrP^C expression is specifically restricted to FDC, whereas in spleens from CD21-Cre *Pmp*^{stop/-}→*Pmp*^{stop/-} mice, FDC lack PrP^C expression. FDC can passively acquire the expression of some surface molecules including MHC class II and complement component C4 [21,32]. However, these data confirm that FDC express high levels of cellular PrP^C on their surfaces and do not simply acquire it from neighbouring cells.

IHC analysis confirmed that the microarchitecture (Figure 3A), size ($P = 0.755$, $n = 32$; Figure 3B) and number ($P = 0.249$, $n = 32$; Figure 3C) of the FDC networks in spleens from mice with *Pmp*-expression restricted to FDC (*Pmp*^{stop/-}→CD21-Cre *Pmp*^{stop/-} mice) were normal when compared to control mice. Other studies have shown that the density of sympathetic nerves can significantly influence the amount of prion accumulation within in the spleen [33]. Quantitative analysis of the relative positioning of FDC and sympathetic nerves showed there were no significant differences in

average distance between these cell populations in spleens from each mouse group (Figure 3D & E; $P < 0.932$, $n = 48$).

FDC-restricted PrP^C-expression is sufficient to sustain prion replication in the spleen

Next, we determined the effect of FDC-restricted *Pmp*-expression on prion replication in the spleen. In this study, the normal cellular form of the prion protein is referred to as PrP^C, and two distinct terms (PrP^{Sc} or PrP^d) are used to describe the disease-specific, abnormal accumulations of PrP that are characteristically found only in prion-affected tissues and considered a reliable biochemical marker for the presence of infectious prions [10]. Disease-specific PrP (PrP^d) accumulations are relatively resistant to proteinase K (PK) digestion, whereas cellular PrP^C is destroyed. Where we were able to confirm this resistance by treatment of samples with PK and subsequent paraffin-embedded tissue (PET) immunoblot analysis [34], PrP^{Sc} is used as a biochemical marker for the presence of prions. Unfortunately, treatment of tissue sections with PK destroys the microarchitecture. Therefore, for IHC analysis tissue sections were fixed and pre-treated to enhance the detection of the disease-specific abnormal accumulations of PrP (PrP^d), whereas cellular PrP^C is denatured by these treatments [4]. We have repeatedly shown in a series of studies that these PrP^d-accumulations occur only in prion-infected tissues, and correlate closely with the presence of ME7 scrapie prions [1,4,13,35–37].

Within weeks after i.p. exposure of WT mice to ME7 scrapie prions, strong accumulations of prion-specific PrP^{Sc} occur upon FDCs within the spleen and are sustained until the terminal stages of disease [1,13,35]. Here, mice were injected i.p. with ME7 scrapie prions and spleens from 4 mice from each group collected 35, 70 and 105 days after exposure. In spleens from control mice (*Pmp*^{+/-}→*Pmp*^{+/-} mice) heavy PrP^d accumulations, consistent with localisation upon FDC, were detected at 70 days after i.p. injection with the scrapie agent and had increased in intensity by 105 days after infection (Figure 4A & B). PET immunoblot confirmed the presence of PrP^{Sc} upon the surfaces of the FDC in spleens from control mice (Figure 4C). Furthermore, in the spleens of *Pmp*^{stop/-}→CD21-Cre *Pmp*^{stop/-} mice in which cellular PrP^C was expressed only on FDC, heavy PrP^{Sc} accumulations were likewise maintained upon FDC (Figure 4A & B). In contrast, in the absence of PrP^C expression by FDC in the spleens of CD21-Cre *Pmp*^{stop/-}→*Pmp*^{stop/-} mice, no PrP^{Sc} accumulations were observed upon FDC. In the spleens of mice with PrP^C-deficient FDC, if PrP was detected at all, it was only occasionally observed within tingibile body macrophages (Figure 4A and B, arrowheads; Figure S1). We also analysed prion infectivity levels in spleens collected 70 days after infection from control mice (*Pmp*^{+/-}→*Pmp*^{+/-} mice) and *Pmp*^{stop/-}→CD21-Cre *Pmp*^{stop/-} mice in which cellular PrP^C was expressed only on FDC (Figure S2; $n = 3$ /group). As anticipated high levels of prion infectivity were observed in each control

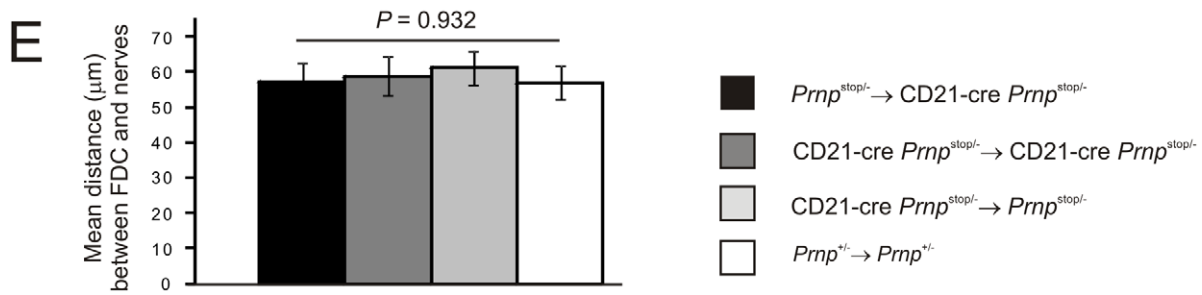
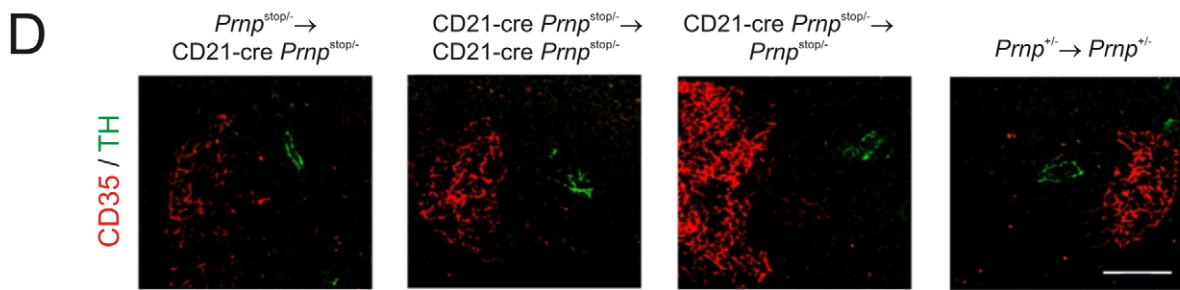
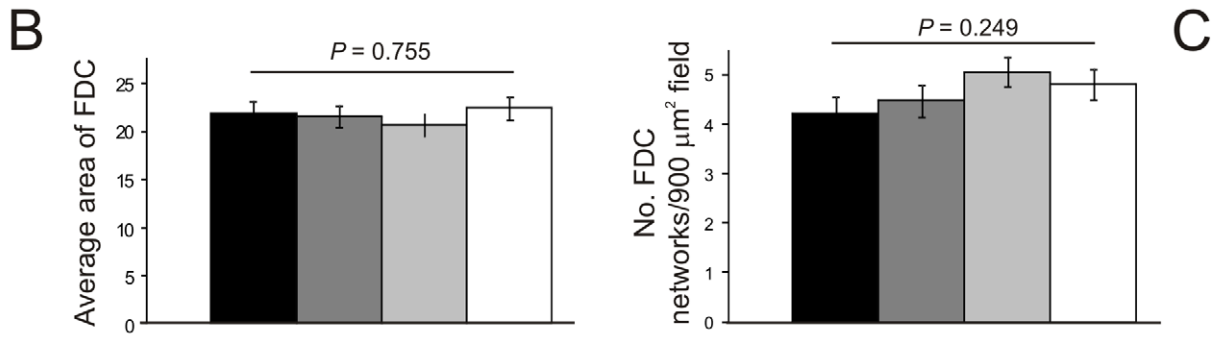
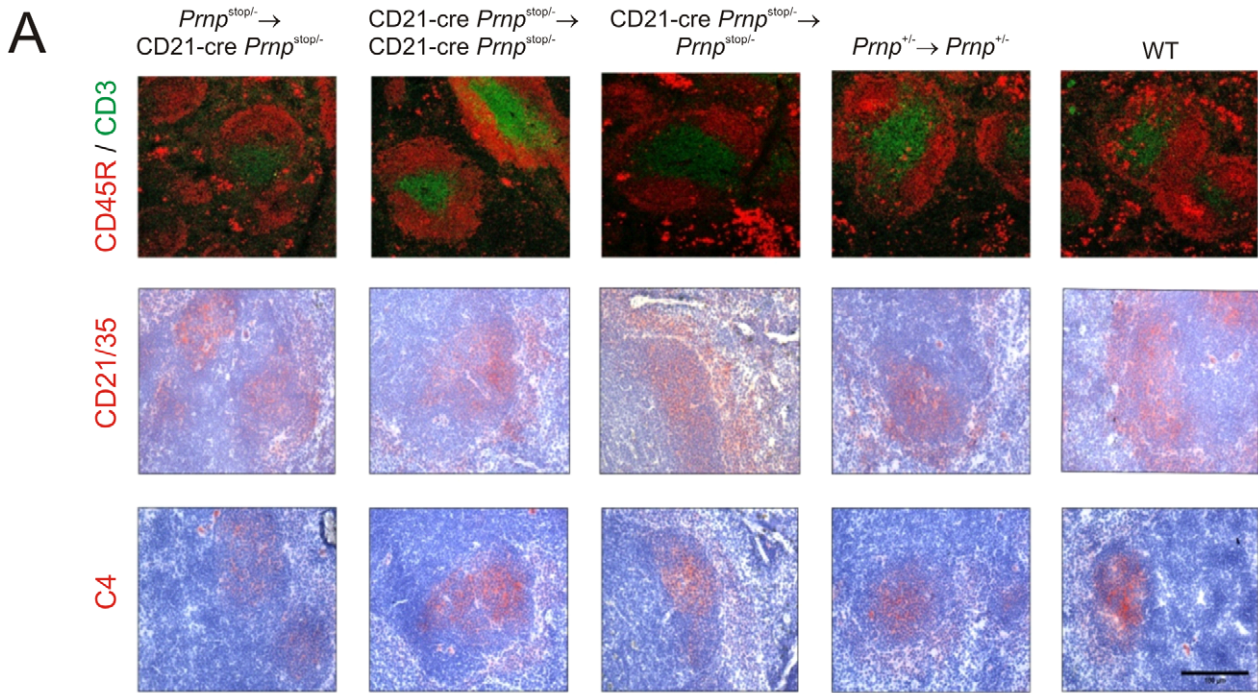


Figure 3. Effect of FDC-restricted PrP^C expression on the spleens of *Pmp^{stop/-}→CD21-Cre Pmp^{stop/-}* mice. A) IHC analysis of the status of FDC networks (C4-binding cells and CD21/CD35⁺ cells; red), B cells expressing CD45R (red), and CD3⁺ T cells (green). Morphometric analysis confirmed that there were no significant difference in the size (B) and number (C) of the CD35⁺ FDC networks in spleens from *Pmp^{stop/-}→CD21-Cre Pmp^{stop/-}*, *CD21-Cre Pmp^{stop/-}→CD21-Cre Pmp^{stop/-}*, *CD21-Cre Pmp^{stop/-}→Pmp^{stop/-}* mice and *Pmp^{+/+}→Pmp^{+/+}* control mice ($n = 32$ FDC networks/group). D and E), Comparison of the sympathetic innervation in spleens from each mouse group. D) IHC detection of TH-positive sympathetic nerves (green) and FDCs (CD35⁺ cells; red). Scale bar, 50 μ m. E) Quantitative analysis of the relative positioning of the FDC and sympathetic nerves showed there were no significant differences in average distance between these cell populations in spleens from each mouse group ($P = 0.932$, $n = 48$ FDC networks/group). For all panels $n = 6$ mice/group.
doi:10.1371/journal.ppat.1002402.g003

spleen. Furthermore, consistent with data above our analysis showed that PrP^C expression only of FDC was sufficient to sustain high levels of prion infectivity within the spleen (Figure S2). These data demonstrate that PrP^C expression only on FDC is sufficient to sustain prion replication in the spleen. In the absence of PrP^C expression on FDC the prions appeared to be scavenged by tingible body macrophages resident within the B cell follicles.

FDC-specific *Pmp*-ablation

Next, mice were created in which *Pmp* expression was specifically ablated in FDC. To do so, *CD21-Cre Pmp^{-/-}* mice were crossed with mice carrying a “floxed” *Pmp* gene (*Pmp^{lox/lox}* mice; [31]). In the progeny *CD21-Cre Pmp^{lox/-}* mice, *Pmp* expression is conditionally ablated in cells expressing Cre recombinase (CD21-expressing FDC and mature B cells). To restrict the *Pmp*-ablation to FDC, *CD21-Cre Pmp^{lox/-}* mice were lethally γ -irradiated and grafted with bone marrow from Cre-deficient *Pmp^{lox/-}* mice (*Pmp^{lox/-}→CD21-Cre Pmp^{lox/-}* mice). We also performed bone marrow transfers from *CD21-Cre Pmp^{lox/-}* donors into *CD21-Cre Pmp^{lox/-}* recipients (*CD21-Cre Pmp^{lox/-}* mice→*CD21-Cre Pmp^{lox/-}* mice), *CD21-Cre Pmp^{lox/-}* donors into Cre-deficient *Pmp^{lox/-}* mice (*CD21-Cre Pmp^{lox/-}*→*Pmp^{lox/-}* mice), and *Pmp^{+/+}* donors into *Pmp^{+/+}* recipients (*Pmp^{+/+}*→*Pmp^{+/+}* mice) as controls (Figure 5A). Spleens, tails and blood from 6 mice from each group were examined 100 days after bone marrow transfusion. PCR analysis of DNA isolated from the spleens, blood and tails of *Pmp^{lox/-}→CD21-Cre Pmp^{lox/-}* mice confirmed that efficient Cre-mediated DNA recombination and *Pmp*-ablation was restricted to the FDC-containing stromal compartment of the spleen (Figure 5B). In *Pmp^{lox/-}→CD21-Cre Pmp^{lox/-}* mice the recombined *Pmp^{stop/-}* allele (*Pmp^{deflox}*) was detected in the spleen, but not blood and tail. Thus these data indicate that in the spleens of *Pmp^{stop/-}→CD21-Cre Pmp^{stop/-}* mice Cre-mediated recombination and *Pmp*-ablation is restricted to FDC and not B cells.

IHC analysis showed that in the spleens of *Pmp^{lox/-}→CD21-Cre Pmp^{lox/-}* mice and *CD21-Cre Pmp^{lox/-}* mice→*CD21-Cre Pmp^{lox/-}* mice FDC did not express PrP^C whereas high levels were associated with TH-positive sympathetic nerves (Figure 5C). In the absence of Cre-recombinase expression by FDC in *CD21-Cre Pmp^{lox/-}→Pmp^{lox/-}* mice, high levels of PrP^C were expressed by FDC and sympathetic nerves (Figure 5C).

Morphometric analysis confirmed that the magnitude of the PrP^C expression co-localized upon the surfaces of FDC in the spleens of *Pmp^{lox/-}→CD21-Cre Pmp^{lox/-}* mice and *CD21-Cre Pmp^{lox/-}* mice→*CD21-Cre Pmp^{lox/-}* mice was substantially lower than that observed upon FDC in spleens from *Pmp^{+/+}→Pmp^{+/+}* control mice ($P < 1 \times 10^{-24}$ and $P < 1 \times 10^{-23}$, respectively, $n = 48$ FDC/group) and not significantly different when compared to background levels (Figure 5D). In contrast, in the absence of Cre-recombinase expression by FDC in *CD21-Cre Pmp^{lox/-}→Pmp^{lox/-}* mice, PrP^C expression was not significantly different from the level observed upon FDC in spleens from *Pmp^{+/+}→Pmp^{+/+}* control mice ($P < 0.106$; Figure 5D). In contrast, morphometric analysis showed that the magnitude of the PrP^C expression co-localized upon the surfaces sympathetic nerves in the spleens of *Pmp^{lox/-}→CD21-Cre*

Pmp^{lox/-}, *CD21-Cre Pmp^{lox/-}*→*CD21-Cre Pmp^{lox/-}* and *CD21-Cre Pmp^{lox/-}→Pmp^{lox/-}* mice was similar to that observed upon sympathetic nerves in spleens from *Pmp^{+/+}→Pmp^{+/+}* control mice ($p = 0.400$, $n = 48$ sympathetic nerves/group). Together, these data confirm that in the spleens of *Pmp^{lox/-}→CD21-Cre Pmp^{lox/-}* mice the *Pmp* ablation is specifically restricted to FDC.

Effect of FDC-specific *Pmp*-ablation on FDC status and splenic microarchitecture

Data in the current study definitively demonstrate that FDC express high levels of PrP^C but the role PrP^C plays in FDC function and homeostasis is not known. IHC analysis showed that the microarchitecture of the FDC networks from *Pmp*-ablated *Pmp^{lox/-}→CD21-Cre Pmp^{lox/-}* mice were normal when compared to control mice (Figure 6A). Furthermore, no significant difference was observed in the size ($P = 0.750$, $n = 32$) and number ($P = 0.713$, $n = 32$) of the FDC networks in spleens from each mouse group (Figure 6B & C, respectively). The relative positioning of the FDC and sympathetic nerves was likewise similar in spleens from each mouse group (Figure 6D & E; $P < 0.765$, $n = 48$).

FDC characteristically trap and retain native antigen on their surfaces in the form of immune complexes, consisting of antigen-antibody and/or complement components. Antigens trapped on the surface of FDC are considered to promote immunoglobulin-isotype class switching, affinity maturation of naïve IgM⁺ B cells and the maintenance of immunological memory [38–42]. Indeed, prions are also considered to be acquired by FDC as complement-opsonized immune complexes [15–18]. To determine whether antigen retention by *Pmp*-ablated FDC was affected six mice from each group were passively immunized with preformed PAP immune complexes, and 24 h later, the presence of FDC-associated immune complexes identified by IHC (Figure 7) and the presence of peroxidase activity (data not shown). No significant difference in the magnitude of immune complex trapping could be detected between FDC from *Pmp*-ablated *Pmp^{lox/-}→CD21-Cre Pmp^{lox/-}* mice and control mice (Figure 7; $P = 0.85$, $n = 40$ /group). Together, these data demonstrate that *Pmp*-ablation does not impair FDC status or their ability to trap and retain immune complexes.

FDC-restricted PrP^C-ablation blocks prion replication in the spleen

Next, the effect of FDC-specific *Pmp*-ablation on prion replication by FDC was determined. Mice were injected i.p. with ME7 scrapie prions and spleens from 4 mice from each group collected 70 days after exposure. As anticipated, heavy PrP^{Sc} (Figure 8A and B) and PrP^{Sc} (Figure 8C) accumulations consistent with localisation upon FDC were detected in spleens from control mice (*Pmp^{+/+}→Pmp^{+/+}* mice) and mice in which *Pmp* was ablated only in mature B cells (*CD21-Cre Pmp^{lox/-}→Pmp^{lox/-}* mice). In the spleens in which cellular PrP^C was ablated only on FDC (*Pmp^{lox/-}→CD21-Cre Pmp^{lox/-}* mice), or FDC and mature B cells (*CD21-Cre Pmp^{lox/-}→CD21-Cre Pmp^{lox/-}* mice), no PrP accumulations were observed upon FDC (Figure 8A–C). Consistent

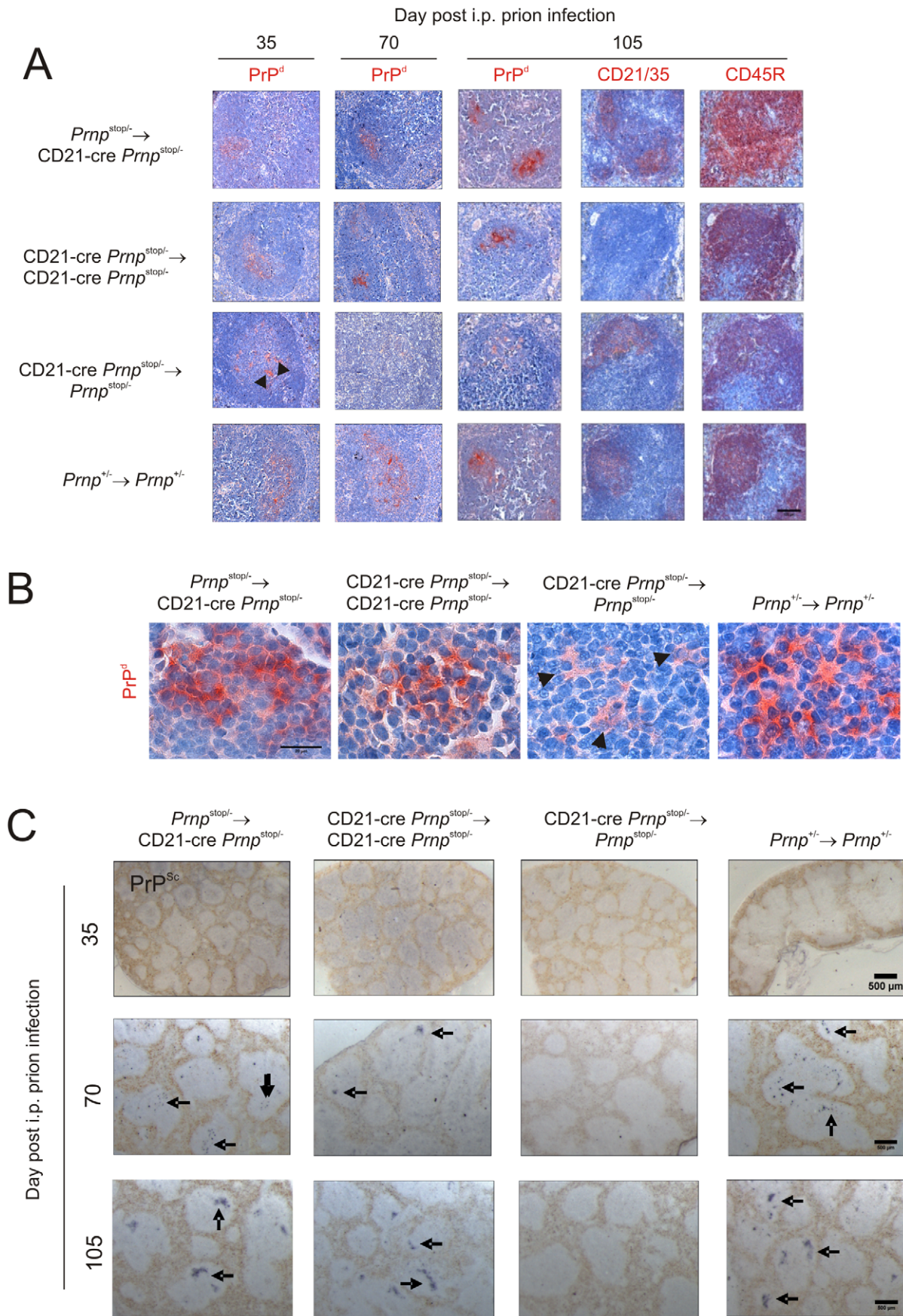


Figure 4. Effect of FDC-restricted PrP^C expression on PrP^{Sc} accumulation in the spleen. Mice were injected i.p. with the ME7 scrapie agent and tissues collected 35, 70 days and 105 days after exposure. A and B) High levels of PrP^d were detected in association with FDC (CD21/35 positive cells) in the B cell follicles (CD45R positive cells) of spleens of mice with PrP^C-expressing FDC: *Pmp^{stop/-}→CD21-Cre Pmp^{stop/-}* mice, CD21-Cre *Pmp^{stop/-}→CD21-Cre Pmp^{stop/-}* mice and *Pmp^{+/+}→Prnp^{+/+}* control mice. B) High magnification images of the sites of PrP^d accumulation (red) at 70 days post-injection with scrapie. Arrowheads show PrP-accumulation within tingible body macrophages. C) Analysis of adjacent sections by PET-immunoblot analysis confirmed the presence of PK-resistant PrP^{Sc} (blue/black). In contrast, no PrP^d or PrP^{Sc} was detected in spleens of CD21-Cre→*Pmp^{stop/-}* mice that lacked PrP^C-expressing FDC. Arrows indicate PrP^{Sc} accumulation upon FDC. A, scale bar = 100 μm. B, scale bar = 20 μm. C, scale bar = 500 μm. For all panels *n* = 4 mice/group.
doi:10.1371/journal.ppat.1002402.g004

with data above (Figure 4), in spleens of mice with PrP^C-deficient FDC PrP accumulations were only occasionally observed within tingible body macrophages (Figure 8A and B, arrowheads; Figure S1). We also analysed prion infectivity levels in spleens from *Pmp^{lox/-}→CD21-Cre Pmp^{lox/-}* mice in which cellular PrP^C expression was ablated only on FDC (Figure S2; *n* = 3). Consistent with data above this analysis showed that in the absence of PrP^C expression only on FDC the accumulation of high levels of prion infectivity in the spleen was blocked (Figure S2). Taken together, these data show that in the specific absence of PrP^C expression FDC are unable to sustain prion replication upon their surfaces and as a consequence the agent is scavenged by tingible body macrophages.

FDC-restricted PrP^C-ablation does not influence prion disease and susceptibility when infection is established directly within the CNS

When mice with PrP^C-ablated FDC (*Pmp^{lox/-}→CD21-Cre Pmp^{lox/-}* mice) were injected intracerebrally (i.c.) with the ME7 scrapie agent strain directly into the CNS all mice succumbed to clinical signs of scrapie approximately 300 days after exposure with incubation periods indistinguishable from those of *Pmp^{+/+}* control mice [43] (*Pmp^{lox/-}→CD21-Cre Pmp^{lox/-}*, 297 ± 4 days, *n* = 4; *Pmp^{+/+}*, 290 ± 4 days, *n* = 5; *P* = 0.386). Histopathological analysis showed that brains from all clinically-affected mice from each group displayed the characteristic spongiform pathology, astrogliosis, microgliosis and PrP^d accumulation typically associated with terminal infection with the ME7 scrapie agent (Figure 9A). Following i.c.-injection with the ME7 scrapie agent, high levels of PrP^{Sc} accumulate upon FDC and are maintained for the duration of the incubation period [13] (Figure 9B and C). However, FDC are not critical for ME7 scrapie pathogenesis when infection is established directly within the CNS [4,13,35,44]. In the spleens from clinically-scrapie affected mice in which PrP^C expression was specifically ablated only on FDC (*Pmp^{lox/-}→CD21-Cre Pmp^{lox/-}* mice), PrP^{Sc} replication upon FDC was also blocked. These data show that FDC do not simply trap and retain prions after their release from infected neurones in the CNS. These data also confirm that the *Pmp*-ablation in *Pmp^{lox/-}→CD21-Cre Pmp^{lox/-}* mice was specific to FDC and had no effect on prion neuropathogenesis and disease susceptibility when the infection was established directly in the CNS.

Effect of FDC-restricted PrP^C-ablation prion neuroinvasion after i.p. exposure

Studies in mice show that efficient prion neuroinvasion from peripheral sites of exposure is dependent upon the presence of FDC in lymphoid tissues [1,4,35,44–46]. Next, the effect of FDC-specific *Pmp*-ablation on prion neuroinvasion via the peritoneal route was determined. Unfortunately, due to the advanced ages of the mice in this experiment, some succumbed to ageing-related inter-current illness. As there was a 100 days interval between the time of lethal γ -irradiation/bone marrow reconstitution and prion infection, many mice were approximately 500–600 days old when

culled. However, most mice with PrP^C-expressing FDC in their spleens succumbed to clinical prion disease after i.p. injection (*Pmp^{+/+}→Pmp^{+/+}* control mice, *n* = 5/7; CD21-Cre *Pmp^{lox/-}→Pmp^{lox/-}* mice, *n* = 3/6; Table S1). Histopathological analysis showed that brains from all clinically-affected mice from these groups displayed the characteristic spongiform pathology, astrogliosis, microgliosis and PrP^d accumulation typically associated with terminal infection with the ME7 scrapie agent (Figure S3, third and fourth columns). In contrast, none of the mice with PrP^C-ablated FDC (*Pmp^{lox/-}→CD21-Cre Pmp^{lox/-}* mice, *n* = 0/6; CD21-Cre *Pmp^{lox/-}→CD21-Cre Pmp^{lox/-}* mice, *n* = 0/7) succumbed to clinical prion disease during their life-spans (Table S1). Although we cannot exclude the possibility that if the clinically-negative mice with PrP^C-ablated FDC mice had lived longer some may have succumbed to clinical prion disease after substantially extended incubation periods, no PrP^d or other characteristic histopathological hallmarks of prion disease were detected in their brains (Figure S3, first two columns). Together, these data suggest that in the specific absence of PrP^C expression on FDC neuroinvasion following peripheral exposure is impaired.

Discussion

These data definitively demonstrate that FDC are essential sites of prion replication in lymphoid tissues. In order to precisely establish the role of FDC in prion pathogenesis two unique compound transgenic mouse models were created in which PrP^C expression was specifically “switched on” or “off” only on FDC. Our data confirm that FDC express high levels of PrP^C and do not simply acquire it from other host cells. Furthermore, we show that following peripheral exposure PrP^C-expressing FDC alone are sufficient to sustain high levels of prion replication in the spleen. Accordingly, when PrP^C-expression was specifically ablated only on FDC prion replication in the spleen was blocked. These data likewise demonstrate that FDC do not simply acquire prions after their release from other infected host cells. Our analysis showed that the effects of *Pmp*-ablation on prion replication in the spleen were specific to FDC and had no effect on prion neuropathogenesis when the infection was established directly in the CNS. In the absence of PrP^C expression on FDC the PrP^{Sc} from the initial inoculum appeared to be scavenged by tingible body macrophages resident within the B cell follicles. Together, these data definitively demonstrate that FDC are the critical early sites of prion replication in lymphoid tissues. This study is the first to demonstrate that the specific ablation of a cellular protein only on FDC, without apparent consequences for FDC status and function, blocks the replication of an important pathogen in the spleen.

FDC reside in the primary B cell follicles and germinal centres of lymphoid tissues and are a completely distinct cell lineage from bone-marrow-derived classical dendritic cells [47–49]. FDC possess many slender and convoluted dendritic processes which provide the FDC with an extremely large surface area. This helps the FDC to efficiently trap and retain large amounts of native antigen in the form of immune complexes, consisting of antigen-

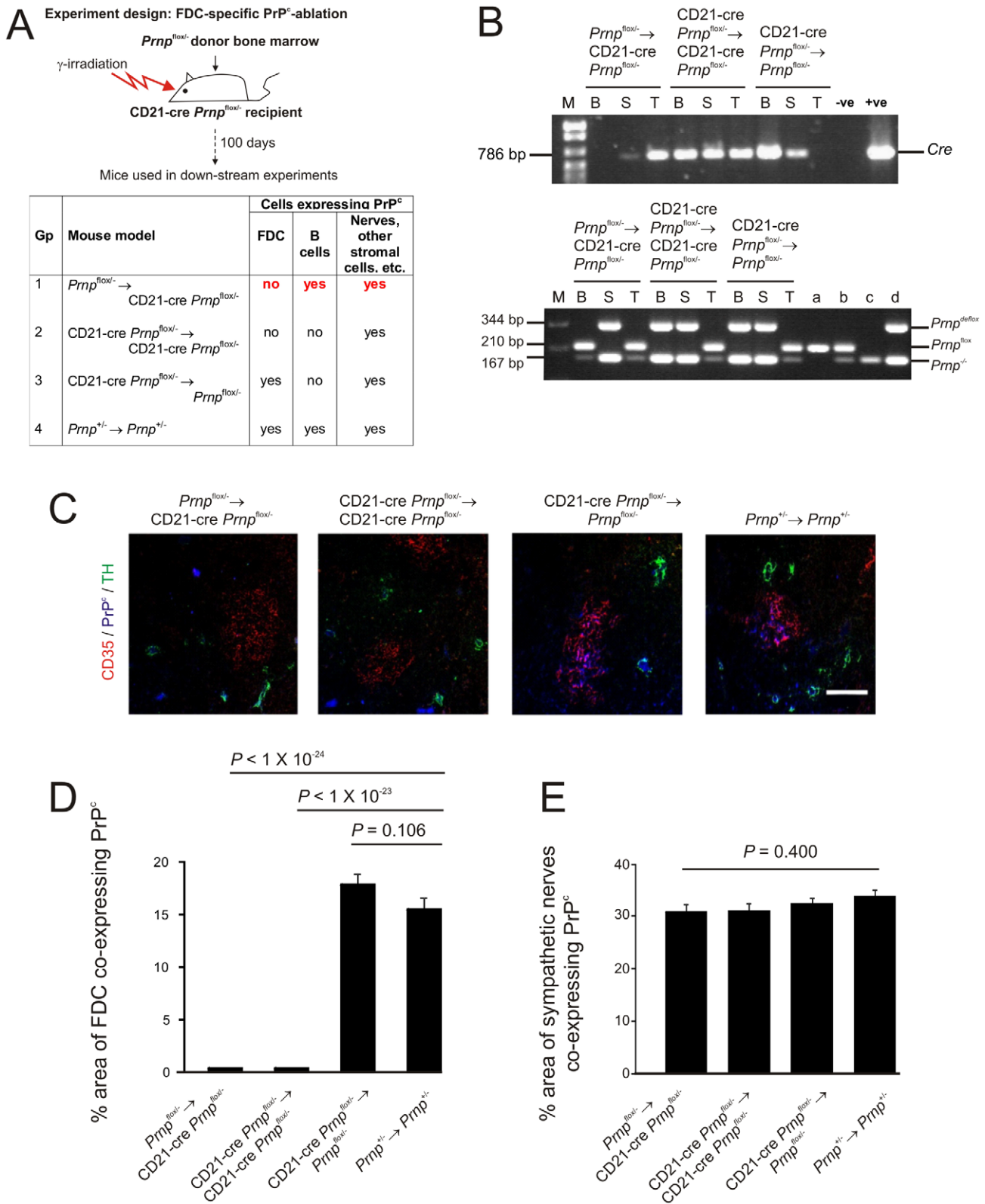


Figure 5. FDC-restricted PrP^c-ablation in the spleens of *Prnp^{flox/flox};CD21-Cre Prnp^{flox/flox}* mice. A) The anticipated distribution of PrP^c expression on FDC and B cells in tissues from each mouse group. B) PCR analysis of DNA isolated from the spleens, blood and tails of *Prnp^{flox/flox};CD21-Cre Prnp^{flox/flox}* mice confirmed that efficient Cre-mediated DNA recombination and *Prnp*-ablation (*Prnp^{deflox}*) was restricted to the FDC-containing stromal compartment of the spleen. Cre-mediated recombination of CD21-expressing lymphocytes was efficiently prevented in these mice by the irradiation and transfer of *Prnp^{flox/flox}* bone marrow as demonstrated by the lack of a *Prnp^{deflox}* band in DNA extracted from blood (lower panel). B, blood; S, spleen; T, tail; M, DNA size markers; a, b, c, d control DNA samples for each transgene combination tested which were (a) *Prnp^{flox/flox}*, (b) *Prnp^{flox/flox}*, (c) *Prnp^{-/-}* and (d) *Prnp^{flox/flox}* with complete recombination of the floxed exon 3. C) IHC analysis of PrP^c expression (blue) by FDC (CD35⁺ cells;

red) and sympathetic nerves (TH⁺ cells, green) confirmed the PrP^C-ablation was restricted to FDC in spleens of *Prnp*^{fllox/-}→CD21-Cre *Prnp*^{fllox/-} mice. Scale bar, 100 μm. D) Morphometric analysis confirmed that the magnitude of the PrP^C expression co-localized upon the surfaces of FDC in the spleens of *Prnp*^{fllox/-}→CD21-Cre *Prnp*^{fllox/-} mice was significantly lower than that observed upon FDC from *Prnp*^{+/-}→*Prnp*^{+/-} control mice ($P < 1.0 \times 10^{-24}$, $n = 48$ FDC networks/group). In contrast, in the absence of Cre-recombinase expression by FDC in CD21-Cre *Prnp*^{fllox/-}→*Prnp*^{fllox/-} mice, PrP^C expression was similar to that observed upon FDC in spleens from *Prnp*^{+/-}→*Prnp*^{+/-} control mice ($P = 0.106$, $n = 48$ FDC networks/group). E) Morphometric analysis confirmed that the magnitude of the PrP^C expression co-localized upon the surfaces sympathetic nerves in the spleens of *Prnp*^{fllox/-}→CD21-Cre *Prnp*^{fllox/-}, CD21-Cre *Prnp*^{fllox/-}→CD21-Cre *Prnp*^{fllox/-} and CD21-Cre *Prnp*^{fllox/-}→*Prnp*^{fllox/-} mice was not significantly different when compared to that observed upon sympathetic nerves in spleens from *Prnp*^{+/-}→*Prnp*^{+/-} control mice ($p = 0.400$, $n = 48$ sympathetic nerves/group). For all panels $n = 6$ mice/group. doi:10.1371/journal.ppat.1002402.g005

antibody and/or complement components. The longevity of FDC ensures that antigen is retained upon their surfaces for long periods [50,51]. Antigens trapped on the surface of FDC are considered to promote immunoglobulin-isotype class switching, affinity maturation of naïve IgM⁺ B cells and the maintenance of immunological memory [38–42]. FDC are also considered to aid the clearance of apoptotic B lymphocytes [52], and play a role in infection with human immunodeficiency virus [53] and the pathogenesis of chronic inflammatory and autoimmune diseases [54] and peripherally-acquired prion infections.

A number of studies have addressed the role of FDC in prion pathogenesis. They show that prion replication in the spleen and subsequent neuroinvasion are both impaired in immunodeficient mice that lack FDC [4,44,45], or following their temporary de-differentiation [1,35,46]. Although the precise identity of FDC precursor cells is unknown, other studies have exploited their non-haematopoietic-origin to address their role in prion pathogenesis. In these bone marrow chimera studies, mismatches were created in *Pmp* expression between the FDC-containing stromal and haematopoietic compartments by grafting bone marrow cells from PrP-deficient (*Pmp*^{-/-}) mice into PrP-expressing wild-type mice, and *vice versa* [13,14]. Using this approach FDC and all other stromal cells were derived from the recipient, whereas lymphocytes and other haematopoietic lineages were derived from the donor cells. Following peripheral exposure prion accumulation upon FDC was only detected in the spleens of mice with a *Pmp*-expressing stromal compartment.

While the above studies clearly show that the presence of FDC is important for prion replication in the spleen, it was not possible to dissociate the *Pmp* expression status of FDC from that of the nervous system and all other non-haematopoietic host-cell populations and therefore precisely characterise the role of FDC in prion neuroinvasion [13,14]. This is important for a number of reasons. Firstly, prion infection can occur within inflammatory PrP^C-expressing stromal cells that are distinct from FDC [23]. Secondly, the FDC's ability to bind exosomes may have lead to the wrong interpretation to be made in earlier studies describing their ontology [55]. Most evidence indicates that FDC do not derive from haematopoietic precursors [29,49]. However, the detection of donor bone marrow derived MHC class-I molecules, and other donor-derived antigens, on the surface of FDC in recipient mice was considered evidence of FDC precursor cells within bone marrow [55]. With hindsight these observations are most likely due to the FDC's capacity to acquire exosome-associated antigens from other cell types [21]. Both PrP^C and PrP^{Sc} can be released from cells in association with exosomes [20]. The possibility, therefore, cannot be excluded that FDC passively acquire prions after their release in exosomes from other infected non-haematopoietic cell populations. Finally, FDC characteristically trap and retain immune complexes on their surfaces. FDC express negligible levels of complement component C4 at the mRNA level but the detection of abundant activated C4 on their surfaces by IHC using mAb FDC-M2 (as used in this study) is indicative of the capture and retention of immune complexes by FDC [32].

Opsonising complement components and cellular CR are likewise considered to play an important role in the retention of prions by FDC [15,16,18]. Thus FDC may simply act as concentrating depots for prion-containing complement-opsonized immune complexes.

The practical hurdles that are encountered when attempting to isolate highly purified FDC from lymphoid tissues have made detailed analysis of their pathobiological functions extremely difficult. The main issues include: contamination with other cell types such as B cells and tingible body macrophages which express MFGE8 (FDC-M1), a common marker used to identify FDC [52,56], low yield, and their dependence on constitutive lymphotoxin β receptor-stimulation to maintain their differentiated state [57]. FDC and mature B cells express high levels of *Cr2* which encodes the complement receptors CR2/CR1 (CD21/35) [18,27]. A previous study used CD21-cre mice to study FDC-specific gene function [27]. In the current study, our data confirm that Cre/loxP-mediated DNA recombination was specific to FDC and mature B cells in CD21-cre mice, and could be restricted to FDC by transfusing the mice with Cre-deficient bone marrow. In some Cre transgenic mouse lines Cre-toxicity is encountered whereby Cre recombinase causes mis-recombination, DNA damage and death of *Cre*-expressing cells [30]. However, our analysis suggested no significant effect of Cre-expression on the number, size and status of FDC networks and B cell follicles. CD21-Cre mice are therefore a powerful *in vivo* tool in which to study FDC-specific gene expression and function.

Expression of PrP^C is mandatory for host cells to sustain prion infection [43]. In the current study to establish whether FDC actively amplify prions a compound transgenic mouse model was created using the CD21-cre mouse line to specifically “switch on” PrP^C expression only on FDC (*Pmp*^{stop/-}→CD21-Cre *Pmp*^{stop/-} mice). As a consequence, only FDC in these mice had the potential to be actively infected with and replicate prions. Our analysis showed that expression of PrP^C only on FDC was sufficient to sustain high levels of PrP^{Sc} accumulation upon FDC in the spleen after peripheral prion exposure. These data definitively demonstrate that FDC are the critical sites of prion replication in lymphoid tissues. Ultrastructural analysis of the cellular compartments within which PrP^d localizes upon/within FDC has failed to show any intracellular accumulation. Instead the PrP^d appears to be restricted to the plasmalemma of their dendritic processes [58]. This implies that early *de novo* PrP^{Sc} conversion occurs upon the surface of FDC.

A second compound transgenic mouse model was created in which PrP^C expression was specifically “switched off” only on FDC (*Pmp*^{fllox/-}→CD21-Cre *Pmp*^{fllox/-} mice). If, as shown above, FDC do actively amplify prions, then one would also expect the specific ablation of PrP^C expression only on FDC to block prion replication in the spleen. Our data confirmed this to be the case. As PrP^C expression in all other host cells (eg: neurones) in these mice was unaffected, these data clearly show that FDC do not simply acquire prions following release from other infected host cells, even in mice with clinical prion disease in the brain. IHC

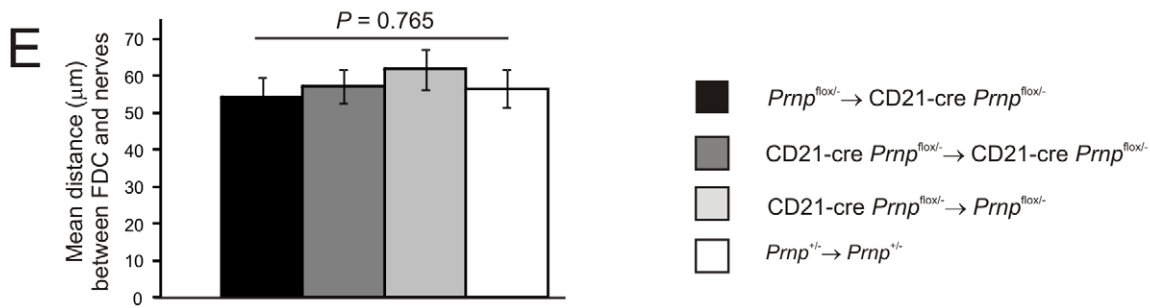
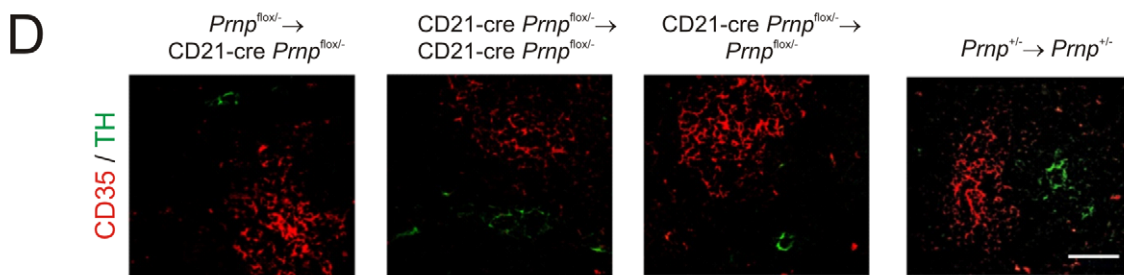
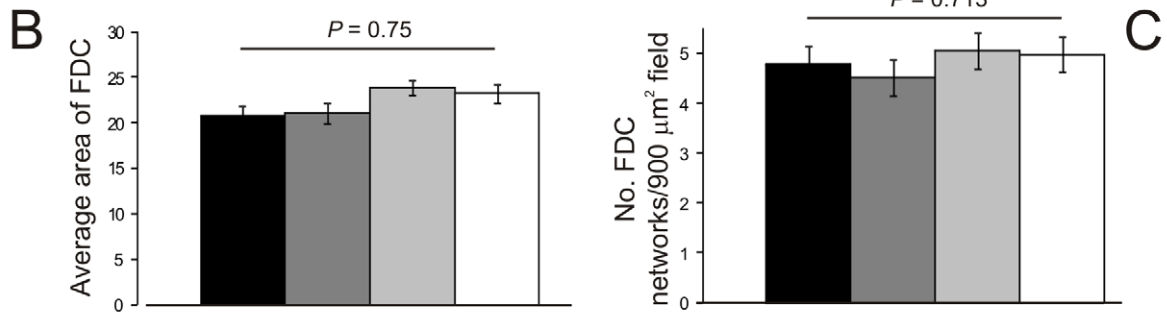
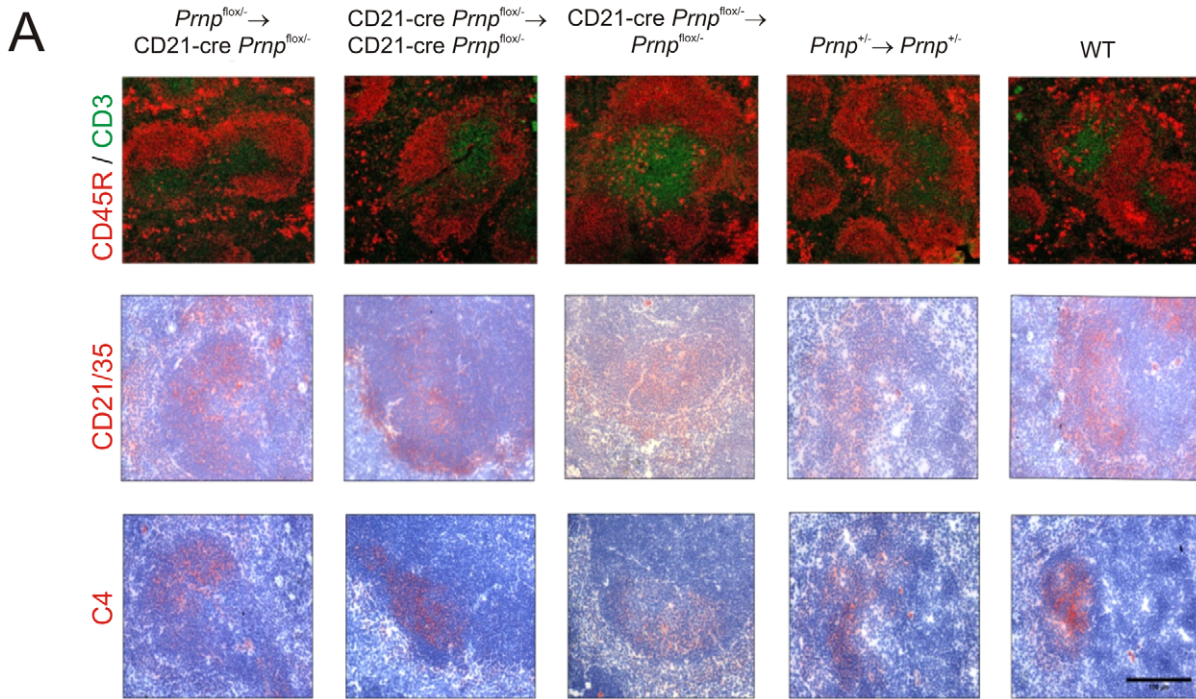


Figure 6. Effect of FDC-restricted PrP^C-ablation on FDC status. A) IHC analysis of the status of FDC (C4-binding cells and CD21/CD35⁺ cells; red), B cells expressing CD45R (red), and CD3⁺ T cells (green). Morphometric analysis confirmed that there were no significant difference in the size (B) and number (C) of the CD35⁺ FDC networks in spleens of mice from each mouse group ($n = 32$ FDC networks/group). D and E), Comparison of the sympathetic innervation in spleens from $Pmp^{lox/-} \rightarrow CD21-Cre Pmp^{lox/-}$, $CD21-Cre Pmp^{lox/-} \rightarrow CD21-Cre Pmp^{lox/-}$, $CD21-Cre Pmp^{lox/-} \rightarrow Pmp^{lox/-}$ mice and $Pmp^{+/-} \rightarrow Pmp^{+/-}$ control mice. D) IHC detection of TH-positive sympathetic nerves (green) and FDCs (CD35⁺ cells; red). Scale bar, 50 μ m. E) Quantitative analysis of the relative positioning of the FDC networks and sympathetic nerves showed there was no significant difference in the average distance between these cell populations in spleens from each mouse group ($P = 0.765$, $n = 48$ FDC networks/group). For all panels $n = 6$ mice/group.
doi:10.1371/journal.ppat.1002402.g006

analysis implied that in the spleens of mice with PrP-deficient FDC the prions appeared to be scavenged by tingible body macrophages resident within the B cell follicles. The lack of detection of PrP^d within tingible body macrophages in the spleens of clinically-affected mice with PrP-deficient FDC (Figure 9) clearly demonstrates that these cells are not alternative sites of replication of ME7 scrapie prions. High levels of prions rapidly accumulate within the spleen and other lymphoid tissues within weeks of peripheral exposure. The magnitude of the prion accumulation within the spleen rapidly reaches a plateau level which is maintained for the duration of the disease [13,44]. The maintenance of this plateau may be the consequence of a competitive state whereby FDC act to amplify prions above the threshold required to achieve neuroinvasion, whereas phagocytic cells such as macrophages act to destroy them [59,60]. Indeed increased numbers of PrP^d-containing tingible body macrophages are found within the B cell follicles of TSE-affected animals [58]. Thus, our data suggest that in the specific absence of PrP^C expression by FDC the initial inoculum is phagocytosed and gradually degraded by mononuclear phagocytes such as tingible body macrophages [59,60]. These data are congruent with data from our earlier study which likewise occasionally detected trace levels of prions from the initial inoculum within tingible body macrophages in the spleens of mice with a PrP^C-deficient FDC-containing stromal compartment [13].

The density of sympathetic nerves can significantly influence the amount of prion accumulation in the spleen [33]. In the current study the distribution of TH-positive sympathetic nerves in the spleens of the FDC-specific gene targeted mouse lines was not adversely affected. Furthermore, when prions were injected directly to the brain, FDC-specific *Pmp* ablation had no influence on the onset of clinical disease or the neuropathology. These data provide strong evidence that the effects of Cre-mediated *Pmp* ablation on prion replication in the spleen were specific to FDC and not due to unregulated ablation of PrP^C expression within the nervous system. In the current study PrP^{Sc} accumulation upon PrP^C-ablated FDC ($Pmp^{lox/-} \rightarrow CD21-Cre Pmp^{lox/-}$ mice) was blocked even in spleens from i.c. injected clinically-scrapie affected mice. These data contrast those reported by Crozet and colleagues [61] which used Tg(OvPrP4) mice that express the ovine *PRNP* gene under the control of the neuron-specific enolase promoter on a murine $Pmp^{-/-}$ background. As a consequence ovine PrP^C is expressed only in neurones. In contrast to data in the current study, when Tg(OvPrP4) mice were injected i.c. with a high dose of natural sheep scrapie PrP^{Sc} was detected in the germinal centres of their spleens. The reasons for this discrepancy are uncertain. However, the expression of PrP^C in the neuronal compartment of Tg(OvPrP4) mice is 2-4X higher than in controls. In the current study in mice in which PrP^C was ablated only on FDC ($Pmp^{lox/-} \rightarrow CD21-Cre Pmp^{lox/-}$ mice) the expression of murine *Pmp* in Cre-deficient cells such as neurones is controlled by the endogenous *Pmp* promoter and expressed at similar levels to controls (Figure 5E). In the presence of increased PrP^C expression on neurones it is plausible that greater prion replication occurred

within the peripheral nervous system, which may have been subsequently trapped on the surface of the FDC and scavenged by macrophages as the prion burden increased. Similarly, hyper-innervation of the spleen likewise leads to increase prion burden in this tissue [33].

In conclusion, our data demonstrate that PrP^C-expressing FDC are the essential sites of prion replication in lymphoid tissues. Indeed, PrP^C-expression on FDC alone was sufficient to sustain high levels of prion replication. In contrast, the specific ablation of PrP^C expression on FDC blocked prion replication. Although FDC have the capacity to bind exosomes and immune complexes which may contain PrP^{Sc}, this finding clearly demonstrates that FDC do not simply passively acquire prions from other infected cell populations such as neurones. Previous data show treatments which impair the status or immune complex-trapping function of FDC reduce prion susceptibility after peripheral exposure [1,16,35,46,62]. The demonstration that *Pmp*-ablation only on FDC blocked splenic prion replication without apparent consequences for FDC status represents a novel opportunity to prevent neuroinvasion by modulation of PrP^C expression on FDC.

Materials and Methods

Ethics statement

All studies using experimental mice and regulatory licences were approved by both The Roslin Institute's and University of Edinburgh's Protocols and Ethics Committees. All animal experiments were carried out under the authority of a UK Home Office Project Licence within the terms and conditions of the strict regulations of the UK Home Office 'Animals (scientific procedures) Act 1986'. Where necessary, anaesthesia appropriate for the procedure was administered, and all efforts were made to minimize harm and suffering. Mice were humanely culled using by a UK Home Office Schedule One method.

Mice

The CD21-Cre [26], ROSA26^{lox/lox} reporter strain [28], $Pmp^{-/-}$ [12] mice and tga20 mice over-expressing PrP^C [63] were generated as described previously. $Pmp^{lox/lox}$ mice have *loxP* sites flanking exon 3 of the *Pmp* gene [31]. $Pmp^{stop/-}$ mice have a floxed β -geo cassette inserted into intron 2 of the *Pmp* gene upstream of exon 3 [31]. Mice were maintained under SPF conditions.

Genotype confirmation by PCR analysis

Prior to their use in experiments, the genotype of each mouse was confirmed by PCR analysis. DNA was prepared from tails, blood and spleens using the DNeasy blood and tissue kit (Qiagen, Crawley, UK) according to the manufacturer's instructions. Where indicated DNA samples were analysed for presence of *Cre*, *LacZ*, $Pmp^{+/+}$, $Pmp^{-/-}$, Pmp^{lox} , recombinant Pmp^{lox} (Pmp^{de-lox}), Pmp^{stop} and recombinant Pmp^{stop} ($Pmp^{stop(R)}$) using the primers listed in Table 1. PCR products were resolved by electrophoresis through a 1.0% agarose gel containing 0.002% GelRed (Biotium, Cambridge Biosciences Ltd, Cambridge, UK).

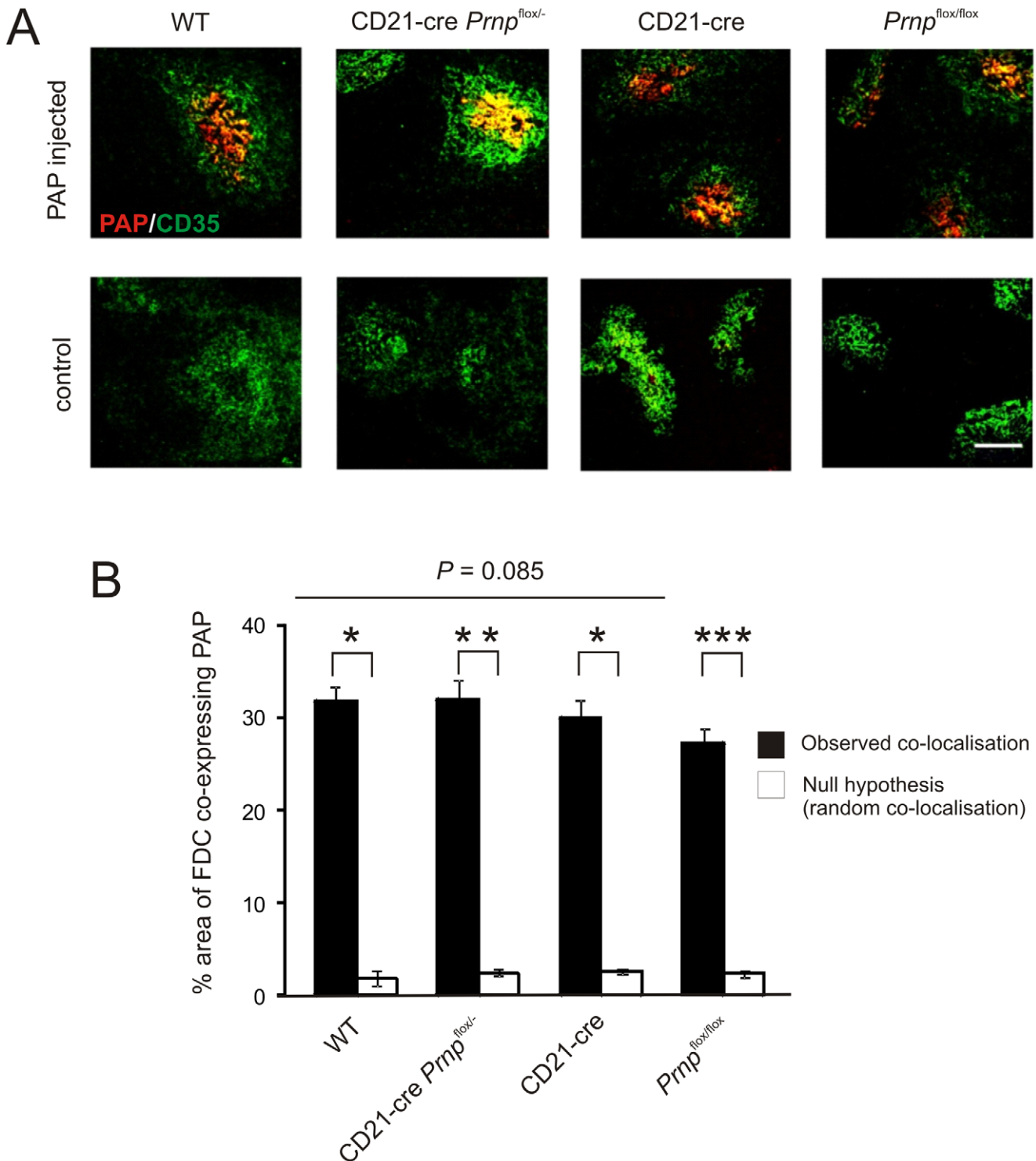


Figure 7. Effect of FDC-restricted PrP^C-ablation on immune complex trapping. A) Mice were passively immunized with preformed PAP immune complexes, and 24 h later, the presence of immune complexes (red) upon FDC (CD35⁺ cells, green) assessed by IHC. Scale bar, 100 μm. B) Morphometric analysis confirmed that the magnitude of the immune complex-trapping co-localized upon the surfaces of FDC from *Prnp*-ablated *Prnp*^{flox/-}→CD21-Cre *Prnp*^{flox/-} mice was not significantly different from that observed in spleens from control mice. This analysis also confirmed that the immune complexes were preferentially associated with FDC in these tissues and significantly greater than the null hypothesis that the pixels were randomly distributed. *, $P < 1 \times 10^{-21}$; **, $P < 1 \times 10^{-32}$; ***, $P < 9 \times 10^{-28}$, $n = 40$ FDC networks/group. For all panels $n = 6$ mice/group. doi:10.1371/journal.ppat.1002402.g007

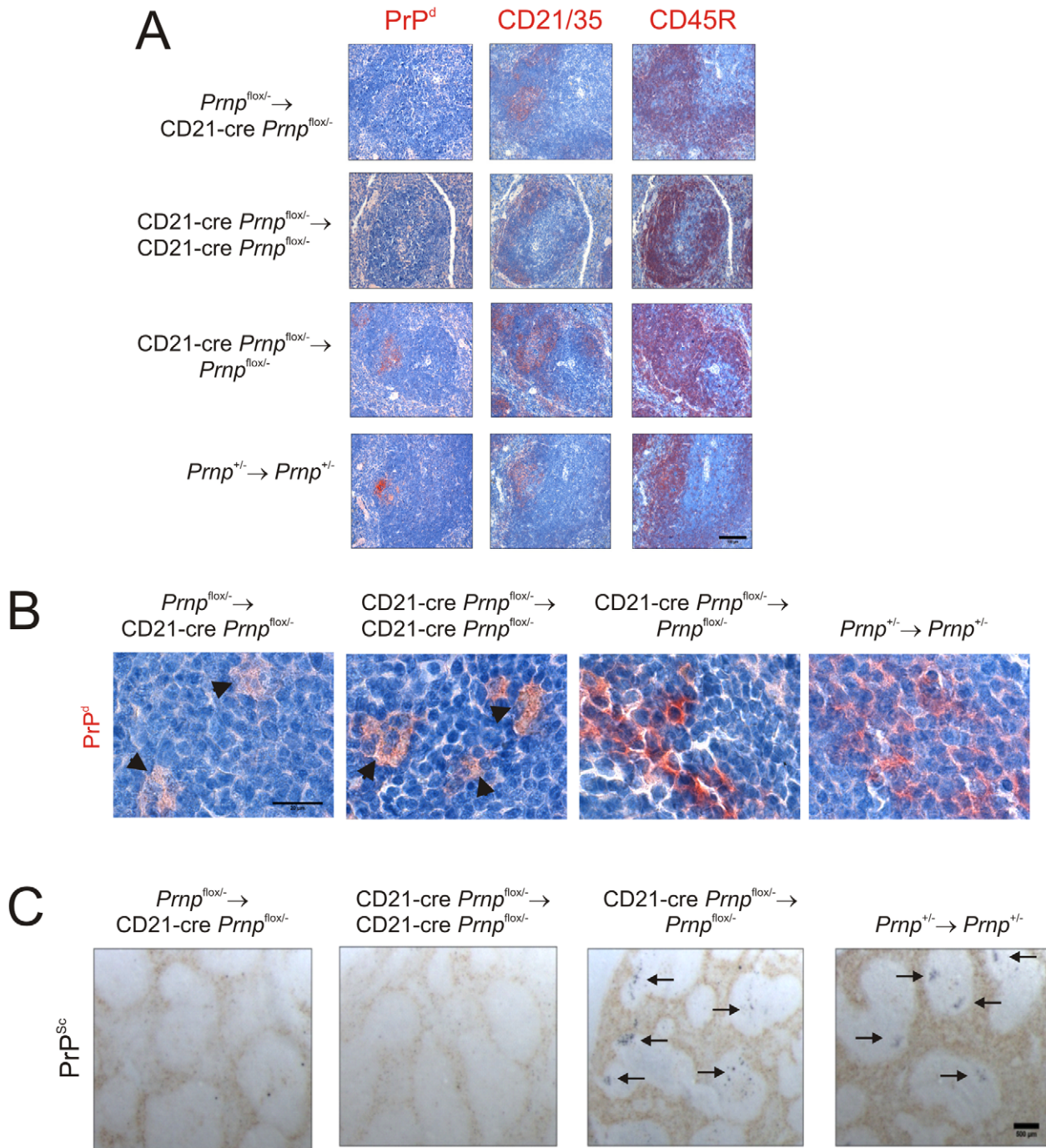


Figure 8. Effect of FDC-restricted PrP^C-ablation on PrP^{Sc} accumulation in the spleen. Mice were injected i.p. with the ME7 scrapie agent and tissues collected 70 days after exposure. A) High levels of PrP^d (red, left-hand column) were detected in association with FDC (red, middle column) in the B cell follicles (red, right-hand column) of spleens from CD21-Cre *Prnp*^{flox/-}->*Prnp*^{flox/-} mice and *Prnp*^{+/-}->*Prnp*^{+/-} control mice that contained PrP^C-expressing FDC. B) High magnification images of the sites of PrP^d accumulation (red) at 70 days post-injection with scrapie. C) PET blot analysis of analysis of adjacent sections by PET-immunoblot analysis confirmed presence of PK-resistant PrP^{Sc} (blue/black). In contrast, no PrP^{Sc} was detected in spleens of *Prnp*^{flox/-}->CD21-Cre *Prnp*^{flox/-} and CD21-Cre *Prnp*^{flox/-}->CD21-Cre *Prnp*^{flox/-} mice that lacked PrP^C-expressing FDC. In the spleens of some of these mice, low levels of PrP^d were occasionally localised within tingible body macrophages (B, arrowheads). A, scale bar = 100 μm. B, scale bar = 20 μm. C, scale bar = 500 μm. Arrows indicate PrP^{Sc} accumulation upon FDC. For all panels *n* = 4 mice/group. doi:10.1371/journal.ppat.1002402.g008

γ-Irradiation and bone-marrow reconstitution

Bone-marrow from the femurs and tibias of donor mice was prepared as single-cell suspensions (3×10^7 – 4×10^7 viable cells/ml) in HBSS (Invitrogen, Paisley, UK). Recipient adult (6–8 weeks old)

mice were γ-irradiated (950 rad) and 24 h later reconstituted with 100 μl bone-marrow by injection into the tail vein. Recipient mice were used in subsequent experiments as described 100 days after bone marrow reconstitution to allow sufficient time for removal of

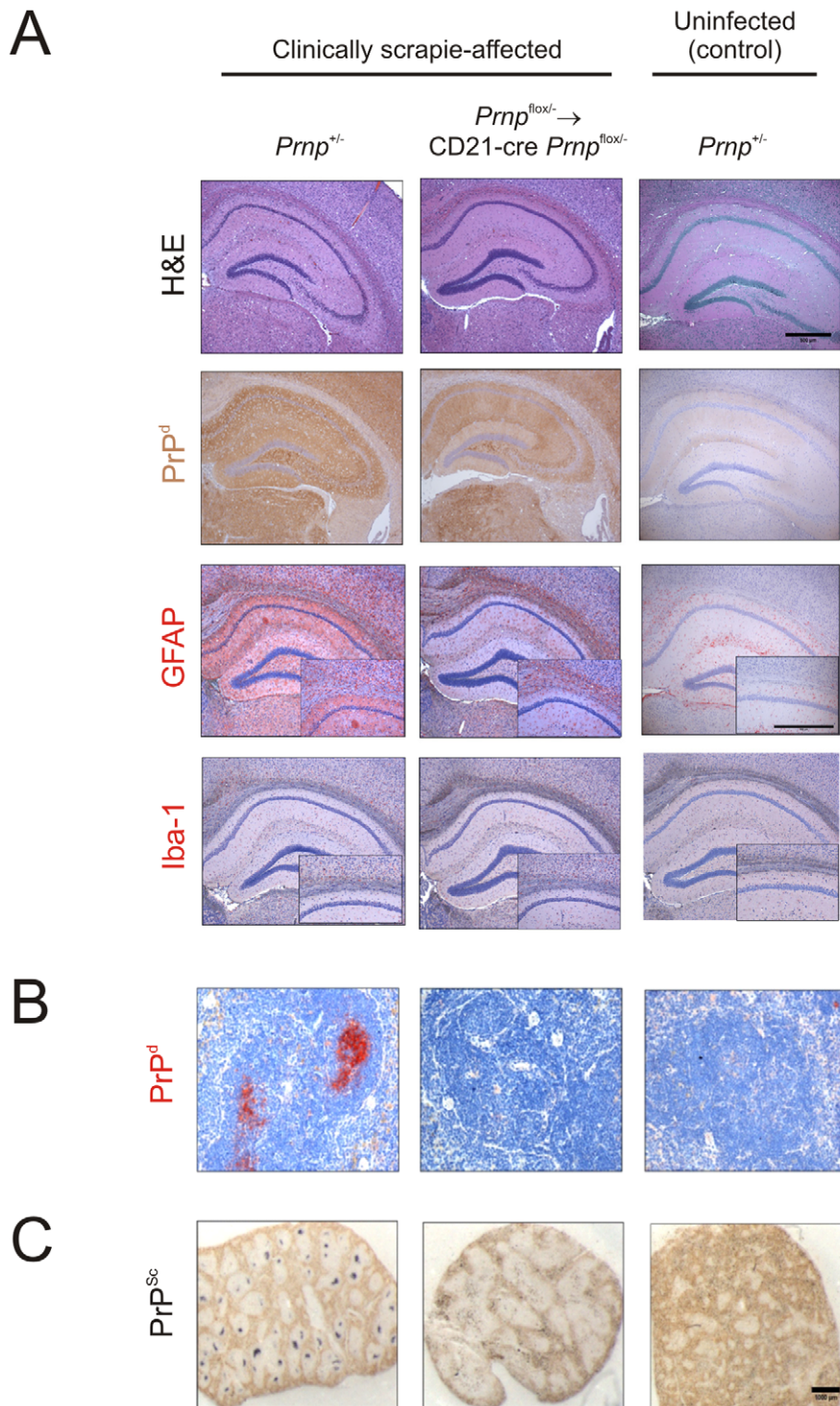


Figure 9. Effect of FDC-restricted PrP^C-ablation on PrP^{Sc} accumulation in the brains and spleens of scrapie-affected mice. Control mice (*Prnp*^{+/-} mice) and *Prnp*^{flox/-} → CD21-Cre *Prnp*^{flox/-} mice that lacked PrP^C-expressing FDC were injected i.c. with the scrapie agent directly into the CNS. Brains and spleens were collected from clinically scrapie-affected mice to compare the neuropathology and cellular sites of PrP^{Sc} accumulation. A) High levels of spongiform pathology (H&E, upper row), heavy accumulations of PrP^d (brown, second row), reactive astrocytes expressing GFAP (brown, third row) and active microglia expressing Iba-1 (brown, bottom row) were detected in the hippocampi of the brains of all clinically scrapie-affected mice. Scale bars, 500 μm. B) High levels of PrP^d (red) were detected in association with FDC in spleens from clinically scrapie-affected control mice that contained PrP^C-expressing FDC. C) PET blot analysis of adjacent sections by PET-immunoblot analysis confirmed the presence of PK-resistant PrP^{Sc} (blue/black). In contrast, no PrP^d or PrP^{Sc} was detected in spleens of *Prnp*^{flox/-} → CD21-Cre *Prnp*^{flox/-} that lacked PrP^C-expressing FDC. Scale bars = 500 μm.

doi:10.1371/journal.ppat.1002402.g009

Table 1. PCR primers used to confirm the genotypes of mice used in this study.

Allele	Details	Primer sequence	Product size/s (bp)
Cre	Fwd	CGAGTGATGAGGTTCCGAAGAACC	786
	Rev	GCTAAGTGCCCTCTACACCTGC	300
LacZ	Fwd	TACCACAGCGGATGGTTCGG	300
	Rev	GTGGTGGTTATGCCGATCGC	
Prnp ^{fllox}	1	AATGGTTAAACTTTCGTTAAGGAT	Prnp ^{de-fllox} 344
	2	GCCGACATCAGTCCACATAG	Prnp ^{fllox} 210
	3	GGTGTGACGCCATGACTTTC	Prnp ^{WT} 167
Prnp ^{null}	Fwd	GCCATCACGAGATTTTCGATT	1,200
	Rev	ATCCCACGATCAGGAAGATG	
Prnp ^{WT}	Fwd	TCATCCACGATCAGGAAGATGAG	600
	Rev	ATGGCGAACCTTGGCTACTGGCTG	
Prnp ^{stop}	1	ACAAATGGGTATGGCTGATTATG	Prnp ^{stop} 1,000
	2	ATGATGATTGAACAAGATGGATTG	Prnp ^{stop(R)} 840
	3	TACCACGAAGTCCGGGATAG	Prnp ^{WT} 750
	4	GCCAGAGGCTAAGGACAACA	

Fwd, forward primer; Rev, reverse primer; (R), Cre-mediated DNA recombined allele.

doi:10.1371/journal.ppat.1002402.t001

long-lived B lymphocyte populations and their replacement from the donor bone marrow.

Histological assessment of LacZ expression

Tissues were first immersed in LacZ fixative [PBS (pH 7.4) containing 2% paraformaldehyde, 0.2% glutaraldehyde, 0.02% Nonidet P40, 0.01% sodium deoxycholate, 5 mM EGTA, 2 mM MgCl₂] and washed in LacZ wash buffer [PBS (pH 7.4) containing 0.02% Nonidet P40, 0.01% sodium deoxycholate, 2 mM MgCl₂]. Tissues were subsequently incubated in 15% (wt/vol) sucrose in PBS overnight followed by a further overnight incubation in 30% (wt/vol) sucrose in PBS and embedded in Tissue-Tek O.C.T. compound (Bayer PLC, Newbury, UK). Serial sections (thickness 8 µm) were cut on cryostat and stained overnight at 37°C with LacZ staining solution (Glycosynth, Warrington, UK). Staining reaction was stopped by washing in LacZ wash buffer followed by dH₂O. Sections were counterstained with nuclear fast red (Vector Laboratories, Peterborough, UK).

Prion exposure and disease monitoring

For i.c. or i.p. exposure mice were injected with 20 µl of a 1% (v/w) scrapie brain homogenate prepared from mice terminally-affected with ME7 scrapie prions (containing approximately 1 × 10⁴ i.c. ID₅₀ units). Following exposure, mice were coded and assessed blindly for signs of clinical disease and culled at a standard clinical endpoint [64]. Survival times were recorded for mice that did not develop clinical signs of disease and were culled when they showed signs of intercurrent disease. Scrapie diagnosis was confirmed blindly on coded sections by histopathological assessment of vacuolation in the brain. For the construction of lesion profiles, vacuolar changes were scored in nine grey-matter areas of brain as described [65]. Where indicated, some four mice from each group were culled at the times indicated post injection with scrapie and tissues taken for further analysis. For bioassay of scrapie agent infectivity, individual half spleens were prepared as 10% (wt/vol) homogenates in physiological saline. Groups of four tga20 indicator

mice were injected i.c. with 20 µl of each homogenate. The scrapie titre in each sample was determined from the mean incubation period in the indicator mice, by reference to a dose/incubation period response curve for ME7 scrapie-infected spleen tissue serially titrated in tga20 mice using the relationship: $y = 9.4533 - 0.0595x$ (y , = log ID₅₀ U/20 µl of homogenate; x , incubation period; $R^2 = 0.9562$). As the expression level of cellular PrP^c controls the prion disease incubation period, tga20 mice overexpressing PrP^c are extremely useful as indicator mice in prion infectivity bioassays as they succumb to disease with much shorter incubation times than conventional mouse strains [63].

IHC and immunofluorescent analyses

Spleens were removed and snap-frozen at the temperature of liquid nitrogen. Serial frozen sections (10 µm in thickness) were cut on a cryostat and immunostained with the following antibodies: FDCs were visualized by staining with mAb 7G6 to detect CR2/CR1 (CD21/CD35; BD Biosciences PharMingen), mAb FDC-M2 to detect C4 (AMS Biotechnology, Oxon, UK) or mAb 8C12 to detect CR1 (CD35; BD Biosciences PharMingen). Cellular PrP^c was detected using PrP-specific polyclonal antibody (pAb) 1B3 [66]. B cells were detected using mAb B220 to detect CD45R (Caltag, Towcester, UK), or anti-CD19 (BD biosciences PharMingen). Marginal zone B cells were detected using mAb 1B1 to detect CD1d (BD Biosciences PharMingen). Sympathetic nerves were detected using tyrosine hydroxylase (TH)-specific pAb (Chemicon Europe).

For the detection of disease-specific PrP (PrP^d) in spleens and brains, tissues were fixed in periodate-lysine-paraformaldehyde fixative and embedded in paraffin wax. Sections (thickness, 6 µm) were deparaffinised, and pre-treated to enhance the detection of PrP^d by hydrated autoclaving (15 min, 121°C, hydration) and subsequent immersion formic acid (98%) for 5 min [67]. Sections were then immunostained with 1B3 PrP-specific pAb. For the detection of EGF-like module-containing mucin-like hormone receptor-like 1 (EMR1)-expressing macrophages, paraffin-embedded spleen sections were micro-waved in citric acid buffer (pH 6.0) for 10 min. Endogenous peroxidase activity was blocked using 1% hydrogen peroxidase in methanol, and macrophages detected using rat mAb F4/80 to detect EMR1 (clone ClA3-1, AbD Serotec). For the detection of astrocytes, brain sections were immunostained with anti-gial fibrillary acidic protein (GFAP; DAKO, Ely, UK). For the detection of microglia, deparaffinised brain sections were first pre-treated with Target Retrieval Solution (DAKO) and subsequently immunostained with anti-ionized calcium-binding adaptor molecule 1 (Iba-1; Wako Chemicals GmbH, Neuss, Germany). Immunolabelling was revealed using HRP-conjugated to the avidin-biotin complex (Novared kit, Vector laboratories, Peterborough, UK). Paraffin-embedded tissue (PET) immunoblot analysis was used to confirm the PrP^d detected by immunohistochemistry was proteinase K (PK)-resistant PrP^{Sc} [34]. Membranes were subsequently immunostained with 1B3 PrP-specific pAb.

For light microscopy, following the addition of primary antibodies, biotin-conjugated species-specific secondary antibodies (Stratech, Soham, UK) were applied followed by alkaline phosphatase or HRP coupled to the avidin/biotin complex (Vector Laboratories). Vector Red (Vector Laboratories) and diaminobenzidine (DAB; Sigma Aldrich, Dorset, UK) were used as substrates, respectively, and sections were counterstained with haematoxylin to distinguish cell nuclei. For fluorescent microscopy, following the addition of primary antibody, species-specific secondary antibodies coupled to Alexa Fluor 488 (green), Alexa Fluor 594 (red) dyes or Alexa Fluor 647 (blue) dyes (Invitrogen, Paisley, UK) were used. Sections were mounted in fluorescent

mounting medium (DakoCytomation) and examined using a Zeiss LSM5 confocal microscope (Zeiss, Welwyn Garden City, UK).

Image analysis

Digital microscopy images were analyzed using ImageJ software (<http://rsbweb.nih.gov/ij/>) as described [68]. Intensity thresholds were first applied and then the number of pixels of each colour (black, red, green, yellow) were then automatically counted and presented as a proportion of the total number of pixels in each area under analysis. The preferential co-localisation of fluorochromes was determined by comparisons of the observed distribution of colours with those predicted by the null hypothesis that each element of positive staining was randomly and independently distributed. Values found to be significantly greater than the null hypothesis confirm significant co-localisation of fluorochromes. Spleens from 6 mice from each group were analyzed. From each spleen, 2 sections were studied and on each section data from 4 individual FDC networks collected. Thus, for each mouse group data from a total of 48 individual FDC were analysed. Similarly, data from 48 images from each group were analyzed to determine the preferential co-localisation of fluorochromes upon TH-positive sympathetic nerves within the spleen. A one-way ANOVA test was then used to compare the null hypothesis (that the pixels were randomly distributed) to the observed levels of co-localisation.

Passive immunization

To assess antigen trapping by FDC *in vivo*, mice were passively immunized by intravenous injection with 100 μ l preformed PAP immune complexes (Sigma). Spleens were removed 24 h later and the presence of FDC-associated immune complexes identified by IHC.

Statistical analyses

Data are presented as mean \pm SE. Unless indicated otherwise, significant differences between samples in different groups were sought by one-way ANOVA. Values of $P < 0.05$ were accepted as significant.

Supporting Information

Figure S1 In the absence of PrP^C expression by follicular dendritic cells prions are scavenged by tingibile body macrophages in the spleen. Mice were injected i.p. with ME7 scrapie prions. Spleens from CD21-Cre *Pmp^{stop/-}→Pmp^{stop/-}* mice (in which cellular PrP^C was expressed only on B cells, upper row), *Pmp^{lox/-}→CD21-Cre Pmp^{lox/-}* mice (with FDC-restricted PrP^C ablation, middle row) and CD21-Cre *Pmp^{lox/-}→CD21-Cre Pmp^{lox/-}* mice (in which PrP^C expression was ablated on FDC and B cells, lower row) were collected 70 days after i.p. infection. Due to the absence of PrP^C-expressing FDC prion replication in these tissues was blocked. However, in the spleens of some of these mice, low levels of PrP^d (left-hand column, red) were occasionally localised within cells with characteristics typical of tingibile body macrophages. These cells contained the remnants of many phagocytosed apoptotic lymphocytes (*tingibile bodies*, arrowheads) and expressed the tissue macrophage marker EGF-like module-containing mucin-like hormone receptor-like 1 (EMR1) detected by mAb F4/80 (right-hand column, brown). Data are representative of spleens from at least 4 mice from each group. Sections are counterstained with haematoxylin (blue). Scale bar, 20 μ m. (PDF)

Figure S2 Follicular dendritic cell-specific PrP^C expression alone is sufficient to sustain high levels of prion infectivity in the spleen. Prion infectivity levels were assayed spleens from control mice (*Pmp^{+/-}→Pmp^{lox/-}* mice), *Pmp^{stop/-}→CD21-Cre Pmp^{stop/-}* mice in which cellular PrP^C was expressed only on FDC and *Pmp^{lox/-}→CD21-Cre Pmp^{lox/-}* mice with FDC-restricted PrP^C ablation ($n = 3$ /group) collected 70 days after i.p. with ME7 scrapie prions. Prion infectivity titres were determined by transmission of tissue homogenates into groups of 4 indicator tga20 mice. Each point represents data derived from an individual spleen. Data below the horizontal line indicate disease incidence in the recipient mice $< 100\%$ and considered to contain trace levels of prion infectivity. High levels of prion infectivity were detected in spleens of control mice and those in which cellular PrP^C was expressed only on FDC (left-hand and middle panels, respectively). However, this accumulation was blocked in spleens with FDC-restricted PrP^C ablation as only trace levels of infectivity were detected (right-hand panel). (PDF)

Figure S3 Effect of FDC-restricted PrP^C-ablation on disease pathogenesis within the brain after i.p. prion exposure. Mice were injected i.p. with ME7 scrapie prions. Brains were collected from clinically scrapie-affected mice and mice which were free of the clinical signs of prion disease at the time of cull and the neuropathology within each brain compared. High levels of spongiform pathology (H&E, upper row), heavy accumulations of PrP^d (brown, second row), reactive astrocytes expressing GFAP (brown, third row) and active microglia expressing Iba-1 (brown, bottom row) were detected in the hippocampi of the brains of all clinically scrapie-affected control mice (right-hand column, $n = 5$) and mice in which PrP^C expression was ablated in B cells only (CD21-Cre *Pmp^{lox/-}→Pmp^{lox/-}* mice, third column, $n = 3$). In contrast, none of the mice with PrP^C-ablated FDC (FDC-restricted, *Pmp^{lox/-}→CD21-Cre Pmp^{lox/-}* mice, first column, $n = 6$; FDC and B cells, CD21-Cre *Pmp^{lox/-}→CD21-Cre Pmp^{lox/-}* mice, second column, $n = 7$) developed clinical signs of prion disease during their life-spans or histopathological signs of prion disease in their brains. Scale bar, = 500 μ m. Clin., presence of clinical signs of scrapie at the time of cull; Path., histopathological detection of spongiform pathology in the brain; dpi, days post i.p. prion infection. (PDF)

Table S1 Effect of FDC-restricted *Pmp* ablation on prion disease pathogenesis after i.p. exposure. (DOCX)

Acknowledgments

We thank Bob Fleming, Nadia Tuzi, Irene McConnell, Fraser Laing, Simon Cumming and the Pathology Services Group (University of Edinburgh, UK) for helpful discussion and excellent technical support; Nathalie Uyttersprot (current address, Artemis Pharmaceuticals GmbH, Germany) and Ari Waisman (Johannes Gutenberg University of Mainz, Germany) for supply of the CD21-cre mice; and Christine Farquhar (University of Edinburgh, UK) for provision of pAb 1B3.

Author Contributions

Conceived and designed the experiments: NAM LM BMB KLB JCM KR JH MB. Performed the experiments: LM KLB NAM. Analyzed the data: LM NAM MB JH. Contributed reagents/materials/analysis tools: MB JCM KR. Wrote the paper: NAM LM BMB KLB JCM KR MB JH.

References

- Mabbott NA, Young J, McConnell I, Bruce ME (2003) Follicular dendritic cell dedifferentiation by treatment with an inhibitor of the lymphotoxin pathway dramatically reduces scrapie susceptibility. *J Virol* 77: 6845–6854.
- Prinz M, Huber G, Macpherson AJS, Heppner FL, Glatzel M, et al. (2003) Oral prion infection requires normal numbers of Peyer's patches but not of enteric lymphocytes. *Am J Pathol* 162: 1103–1111.
- Horiuchi M, Furuoka H, Kitamura N, Shinagawa M (2006) A lymphoplasia mice are resistant to prion infection via oral route. *Jap J Vet Res* 53: 149–157.
- Glaysher BR, Mabbott NA (2007) Role of the GALT in scrapie agent neuroinvasion from the intestine. *J Immunol* 178: 3757–3766.
- Andreoletti O, Berthon P, Marc D, Sarradin P, Grosclaude J, et al. (2000) Early accumulation of PrP^{Sc} in gut-associated lymphoid and nervous tissues of susceptible sheep from a Romanov flock with natural scrapie. *J Gen Virol* 81: 3115–3126.
- Sigurdson CJ, Williams ES, Miller MW, Spraker TR, O'Rourke KI, et al. (1999) Oral transmission and early lymphoid tropism of chronic wasting disease PrP^{Sc} in mule deer fawns (*Odocoileus hemionus*). *J Gen Virol* 80: 2757–2764.
- Hilton D, Fathers E, Edwards P, Ironside J, Zajicek J (1998) Prion immunoreactivity in appendix before clinical onset of variant Creutzfeldt-Jakob disease. *Lancet* 352: 703–704.
- Wilke G, Steinhilber G, Grun J, Berek C (2010) In silico subtraction approach reveals a close lineage relationship between follicular dendritic cells and BP3^{hi} stromal cells isolated from SCID mice. *Eur J Immunol* 40: 2165–2173.
- Beekes M, McBride PA (2007) The spread of prions through the body in naturally acquired transmissible spongiform encephalopathies. *FEBS J* 274: 588–605.
- Bolton DC, McKinley MP, Prusiner SB (1982) Identification of a protein that purifies with the scrapie prion. *Science* 218: 1309–1311.
- Legname G, Baskakov IV, Nguyen H-OB, Riesner D, Cohen FE, et al. (2004) Synthetic mammalian prions. *Science* 305: 673–676.
- Manson JC, Clarke AR, Hooper ML, Aitchison L, McConnell I, et al. (1994) 129/Ola mice carrying a null mutation in PrP that abolishes mRNA production are developmentally normal. *Mol Neurobiol* 8: 121–127.
- Brown KL, Stewart K, Ritchie D, Mabbott NA, Williams A, et al. (1999) Scrapie replication in lymphoid tissues depends on PrP-expressing follicular dendritic cells. *Nat Med* 5: 1308–1312.
- Klein MA, Frigg R, Raeber AJ, Flechsig E, Hegyi I, et al. (1998) PrP expression in B lymphocytes is not required for prion neuroinvasion. *Nat Med* 4: 1429–1433.
- Klein MA, Kaeser PS, Schwarz P, Weyd H, Xenarios I, et al. (2001) Complement facilitates early prion pathogenesis. *Nat Med* 7: 488–492.
- Mabbott NA, Bruce ME, Botto M, Walport MJ, Pepys MB (2001) Temporary depletion of complement component C3 or genetic deficiency of C1q significantly delays onset of scrapie. *Nat Med* 7: 485–487.
- Mabbott NA, Bruce ME (2004) Complement component C5 is not involved in scrapie pathogenesis. *Immunobiology* 209: 545–549.
- Zabel MD, Heikenwalder M, Prinz M, Arrighi I, Schwarz P, et al. (2007) Stromal complement receptor CD21/35 facilitates lymphoid prion colonization and pathogenesis. *J Immunol* 179: 6144–6152.
- Denzer K, Kleijmeer MJ, Heijnen HFG, Stoorvogel W, Geuze HJ (2000) Exosome: from internal vesicle of the multivesicular body to intercellular signalling device. *J Cell Sci* 113: 3365–3374.
- Fevrier B, Vilette D, Archer F, Loew D, Faigle W, et al. (2004) Cells release prions in association with exosomes. *Proc Natl Acad Sci USA* 101: 9683–9688.
- Denzer K, van Eijk M, Kleijmeer MJ, Jakobson E, de Groot C, et al. (2000) Follicular dendritic cells carry MHC class II-expressing microvesicles at their surface. *J Immunol* 165: 1259–1265.
- Mohan J, Brown KL, Farquhar CF, Bruce ME, Mabbott NA (2004) Scrapie transmission following exposure through the skin is dependent on follicular dendritic cells in lymphoid tissues. *J Dermatol Sci* 35: 101–111.
- Heikenwalder M, Kurrer MO, Margalith I, Kranich J, Zeller N, et al. (2008) Lymphotoxin-dependent prion replication in inflammatory stromal cells of granulomas. *Immunity* 29: 998–1008.
- Thomzig A, Kratzel C, Lenz G, Krüger D, Beekes M (2003) Widespread PrP^{Sc} accumulation in muscles of hamsters orally infected with scrapie. *EMBO Rep* 4: 530–533.
- Šimák J, Holanda K, D'Agnillo F, Janota J, Vostal JG (2002) Cellular prion protein in expressed on endothelial cells and is released during apoptosis on membrane microparticles found in human plasma. *Transfusion* 42: 334–342.
- Kraus M, Alimzhanov MB, Rajewsky N, Rajewsky K (2004) Survival of resting mature B lymphocytes depends on BCR signaling via the Ig α / β heterodimer. *Cell* 117: 787–800.
- Victoratos P, Lagnel J, Tzima S, Alimzhanov MB, Rajewsky K, et al. (2006) FDC-specific functions of p55TNFR and IKK2 in the development of FDC networks and of antibody responses. *Immunity* 24: 65–77.
- Mao X, Fujiwara Y, Orkin SH (1999) Improved reporter strain for monitoring Cre recombinase-mediated DNA excisions in mice. *Proc Natl Acad Sci, USA* 96: 5037–5042.
- Tkachuk M, Bolliger S, Rytzel B, Pluschke G, Banks TA, et al. (1998) Crucial role of tumour necrosis factor receptor 1 expression on nonhematopoietic cells for B cell localization within the splenic white pulp. *J Exp Med* 187: 469–477.
- Schmidt-Supprian M, Rajewsky K (2007) Vagaries of conditional gene targeting. *Nat Immunol* 8: 665–668.
- Tuzi NL, Clarke AR, Bradford B, Aitchison L, Thomson V, et al. (2004) Cre-loxP mediated control of PrP to study transmissible spongiform encephalopathy diseases. *Genesis* 40: 1–6.
- Taylor PR, Pickering MC, Kosco-Vilbois MH, Walport MJ, Botto M, et al. (2002) The follicular dendritic cell restricted epitope, FDC-M2, is complement C4; localization of immune complexes in mouse tissues. *Eur J Immunol* 32: 1883–1896.
- Glatzel M, Heppner FL, Albers KM, Aguzzi A (2001) Sympathetic innervation of lymphoreticular organs is rate limiting for prion neuroinvasion. *Neuron* 31: 25–34.
- Schulz-Schaeffer WJ, Tschoke S, Kranefuss N, Drose W, Hause-Reiter D, et al. (2000) The paraffin-embedded tissue blot detects PrP^{Sc} early in the incubation time in prion diseases. *Am J Pathol* 156: 51–56.
- Mabbott NA, Mackay F, Minns F, Bruce ME (2000) Temporary inactivation of follicular dendritic cells delays neuroinvasion of scrapie. *Nat Med* 6: 719–720.
- Raymond CR, Aucouturier P, Mabbott NA (2007) *In vivo* depletion of CD11c⁺ cells impairs scrapie agent neuroinvasion from the intestine. *J Immunol* 179: 7758–7766.
- Brown KL, Wathne GJ, Sales J, Bruce ME, Mabbott NA (2009) The effects of host age on follicular dendritic cell status dramatically impair scrapie agent neuroinvasion in aged mice. *J Immunol* 183: 5199–5207.
- Fu Y-X, Molina H, Matsumoto M, Huang G, Min J, et al. (1997) Lymphotoxin- α (LT α) supports development of splenic follicular structure that is required for IgG response. *J Exp Med* 185: 2111–2120.
- Fu Y-X, Huang G, Wang Y, Chaplin DD (1998) B lymphocytes induce the formation of follicular dendritic cell clusters in a lymphotoxin α -dependent fashion. *J Exp Med* 187: 1009–1018.
- Endres R, Alimzhanov MB, Plitz T, Futterer A, Kosco-Vilbois MH, et al. (1999) Mature follicular dendritic cell networks depend on expression of lymphotoxin β receptor by radioresistant stromal cells and of lymphotoxin β and tumour necrosis factor by B cells. *J Exp Med* 189: 159–168.
- Fu Y-X, Huang G, Wang Y, Chaplin DD (2000) Lymphotoxin- α -dependent spleen microenvironment supports the generation of memory B cells and is required for their subsequent antigen-induced activation. *J Immunol* 164: 2508–2514.
- Aydar Y, Sukumar A, Szakal AK, Tew JG (2005) The influence of immune complex-bearing follicular dendritic cells on the IgM response, Ig class switching, and production of high affinity IgG. *J Immunol* 174: 5358–5366.
- Manson JC, Clarke AR, McBride PA, McConnell I, Hope J (1994) PrP gene dosage determines the timing but not the final intensity or distribution of lesions in scrapie pathology. *Neurodegeneration* 3: 331–340.
- Mabbott NA, Williams A, Farquhar CF, Pasparkis M, Kollias G, et al. (2000) Tumor necrosis factor- α -deficient, but not interleukin-6-deficient, mice resist peripheral infection with scrapie. *J Virol* 74: 3338–3344.
- Prinz M, Montrasio F, Klein MA, Schwarz P, Priller J, et al. (2002) Lymph nodal prion replication and neuroinvasion in mice devoid of follicular dendritic cells. *Proc Natl Acad Sci USA* 99: 919–924.
- Montrasio F, Frigg R, Glatzel M, Klein MA, Mackay F, et al. (2000) Impaired prion replication in spleens of mice lacking functional follicular dendritic cells. *Science* 288: 1257–1259.
- Shortman K, Liu Y-J (2002) Mouse and human dendritic cell subtypes. *Nat Rev Immunol* 2: 151–161.
- Imazeki N, Senoo A, Fuse Y (1992) Is the Follicular Dendritic Cell a Primarily Stationary Cell? *Immunology* 76: 508–510.
- Mabbott NA, Bailie JK, Kobayashi A, Donaldson DS, Ohmori H, et al. (2011) Expression of mesenchyme-specific gene signatures by follicular dendritic cells: insights from the meta-analysis of microarray data from multiple mouse cell populations. *Immunology* 133: 482–498.
- Mandel TE, Phipps RP, Abbot A, Tew JG (1980) The follicular dendritic cell: long term antigen retention during immunity. *Immunol Review* 53: 29–59.
- Suzuki K, Grigороva I, Phan TG, Kelly LM, Cyster JG (2009) Visualizing B cell capture of cognate antigen from follicular dendritic cells. *J Exp Med* 206: 1485–1493.
- Kranich J, Krautler NJ, Heinen E, Polymenidou M, Bridel C, et al. (2008) Follicular dendritic cells control engulfment of apoptotic bodies by secreting Mfge8. *J Exp Med* 205: 1293–1302.
- Burton GF, Brandon FK, Estes JD, Thacker TC, Gartner S (2002) Follicular dendritic cell contributions to HIV pathogenesis. *Sem Immunol* 14: 275–284.
- Gommerman JL, Browning JL (2003) Lymphotoxin/LIGHT, lymphoid microenvironments and autoimmune disease. *Nat Rev Immunol* 3: 642–654.
- Kapasi ZF, Qin D, Kerr WG, Kosco-Vilbois MH, Schultz LD, et al. (1998) Follicular dendritic cell (FDC) precursors in primary lymphoid tissues. *J Immunol* 160: 1078–1084.
- Hanamaya R, Tanaka M, Miyasaka K, Azozsa K, Koike M, et al. (2004) Autoimmune disease and impaired uptake of apoptotic cells in MFG-E8-deficient mice. *Science* 304: 1147–1150.
- Mackay F, Browning JL (1998) Turning off follicular dendritic cells. *Nature* 395: 26–27.

58. McGovern G, Mabbott NA, Jeffrey M (2009) Scrapie affects the maturation cycle and immune complex trapping by follicular dendritic cells in mice. *PLoS One* 4: e8186.
59. Carp RI, Callahan SM (1982) Effect of mouse peritoneal macrophages on scrapie infectivity during extended in vitro incubation. *Intervirology* 17: 201–207.
60. Maignien T, Shakweh M, Calvo P, Marcé D, Salès N, et al. (2005) Role of gut macrophages in mice orally contaminated with scrapie or BSE. *Int J Pharmaceutics* 298: 293–304.
61. Crozet C, Lezmi S, Flamant F, Samarut J, Baron T, et al. (2007) Peripheral circulation of the prion infectious agent in transgenic mice expressing the ovine prion protein in neurons only. *J Infect Dis* 195: 997–1006.
62. Mohan J, Bruce ME, Mabbott NA (2005) Follicular dendritic cell dedifferentiation reduces scrapie susceptibility following inoculation via the skin. *Immunology* 114: 225–234.
63. Fischer M, Rulicke T, Raeber A, Sailer A, Moser M, et al. (1996) Prion protein (PrP) with amino-proximal deletions restoring susceptibility of PrP knockout mice to scrapie. *EMBO J* 15: 1255–1264.
64. Fraser H, Dickinson AG (1973) Agent-strain differences in the distribution and intensity of grey matter vacuolation. *J Comp Pathol* 83: 29–40.
65. Fraser H, Dickinson AG (1968) The sequential development of the brain lesions of scrapie in three strains of mice. *J Comp Pathol* 78: 301–311.
66. Farquhar CF, Somerville RA, Ritchie LA (1989) Post-mortem immunodiagnosis of scrapie and bovine spongiform encephalopathy. *J Virol Met* 24: 215–222.
67. McBride P, Eikelenboom P, Kraal G, Fraser H, Bruce ME (1992) PrP protein is associated with follicular dendritic cells of spleens and lymph nodes in uninfected and scrapie-infected mice. *J Pathol* 168: 413–418.
68. Inman CF, Rees LEN, Barker E, Haverson K, Stokes CR, et al. (2005) Validation of computer-assisted, pixel-based analysis of multiple-colour immunofluorescence histology. *J Immunol Met* 302: 156–167.